J. International Journal of Applied Pharmaceutics

ISSN- 0975-7058 Vol 18, Issue 3, 2026

Review Article

LEVERAGING IN SILICO MODELS FOR THE RATIONAL DESIGN OF GRAPHENE QUANTUM DOT-BASED DRUG DELIVERY SYSTEMS FOR BREAST CANCER: AN APPLIED PHARMACEUTICS PERSPECTIVE

JIMI K. J.[1], VAISHNAVI GURURAJ PAGE[1], ABHILASH RAVIKUMAR[2], AMRITA THAKUR[1], ANIL KUMAR S.[1*]

[1]Department of Physical Sciences, Amrita School of Engineering, Amrita Vishwa Vidyapeetham, Bengaluru-560035, (Karnataka) India.
[2]Nanoelectronics Research Laboratory, Department of Electronics and Communication Engineering, Amrita School of Engineering, Amrita Vishwa Vidyapeetham, Bengaluru-560035, (Karnataka) India
[*]Corresponding author: Anil Kumar S.; [*]Email: s_anilkumar@blr.amrita.edu

Received: 06 Nov 2025, Revised and Accepted: 14 Mar 2026

ABSTRACT

Delivering chemotherapy to aggressive forms of breast cancers including triple-negative breast cancer (TNBC) is hindered by poor drug bioavailability, limited tumor penetration, and off-target toxicity. While conventional carriers often struggle with biological barriers, Graphene Quantum Dots (GQDs) offer a versatile solution. This review examines how computational design-specifically density functional theory (DFT) and molecular dynamics (MD) simulations-is accelerating the development of GQDs as precision nanocarriers. Due to their ultrasmall size, GQDs penetrate deep into the dense tumor microenvironment (TME), while surface functionalization with ligands like folic acid ensures selective targeting. These "smart" carriers can be engineered for pH-responsive drug release, triggered by the acidic conditions of the tumor to minimize side effects. Beyond delivery, the intrinsic fluorescence and high drug-loading capacity of GQDs enable a "theranostic" approach, combining real-time imaging with therapy. By integrating in silico modeling with nanotechnology, these advancements point toward more adaptive, personalized treatments for TNBC.

Keywords: Graphene quantum dots, Breast cancer therapy, Tumor microenvironment, Targeted drug delivery, Theranostics, pH-responsive nanoparticles

DOI: https://dx.doi.org/10.22159/ijap.2026v18i3.57396 Journal homepage: https://innovareacademics.in/journals/index.php/ijap

INTRODUCTION

Breast cancer is a complex and multifaceted disease that occurs when cells in the breast tissue begin to multiply uncontrollably forming a tumor [1-5]. It is by far the most diagnosed cancer in women worldwide and comprises several different subtypes, each characterized by different molecular features that affect disease progression and response to therapy. These subtypes are mainly classified on the basis of the presence or absence of three important receptors present on the surface of the cancer cells: estrogen receptors (ER), progesterone receptors (PR) and human epidermal growth factor receptor 2 (HER2) [6-8].

Hormone receptor-positive breast cancers, which express ER and/or PR, are caused by the body's natural hormones and respond well to hormone-blocking therapies. HER2-positive cancers, characterized by an overexpression of the HER2 protein, are more aggressive in their growth but can be treated using targeted therapies such as trastuzumab. Accounting for between 15-20% of all diagnoses, triple-negative breast cancer (TNBC) is an aggressive subtype that disproportionately affects younger women and women with the breast cancer mutation, BRCA1 [9, 10]. Unlike other types of breast cancer, TNBC is characterized by what it does not have in terms of receptors (ER, PR and HER2), which are the targets for targeted therapies, making it especially difficult to cure the cancer and increasing the likelihood of recurrence and metastasis [11]. While targeted therapies have improved outcomes for other breast cancer subtypes, challenges such as drug resistance, severe side effects, and limited treatment options for triple-negative breast cancer persist [12]. These hurdles really drive home the need for smarter therapies that can deliver drugs more precisely and give doctors real-time insight into how well treatments are working. This has led to the emergence of theranostics, a promising approach that integrates therapy and diagnostics [13-16].

Recently, Ko *et al.* demonstrated that herceptin-labeled GQD nanocarriers loaded with β-cyclodextrin offer a multifunctional theranostic platform for treating HER2-overexpressing breast cancer (fig. 1) [13]. The roleofherceptin is to facilitate selective targeting of cancer cells and thereby limiting the off-target effects while β-cyclodextrin offers loading sites for the hydrophobic drug doxorubicin (DOX). Under acidic conditions, DOX is released on to the tumor microenvironment (TME) in a controlled fashion to arrest cancer propagation. Further the presence of nanocarriers help in diagnosis as well due to the blue colour they emit.

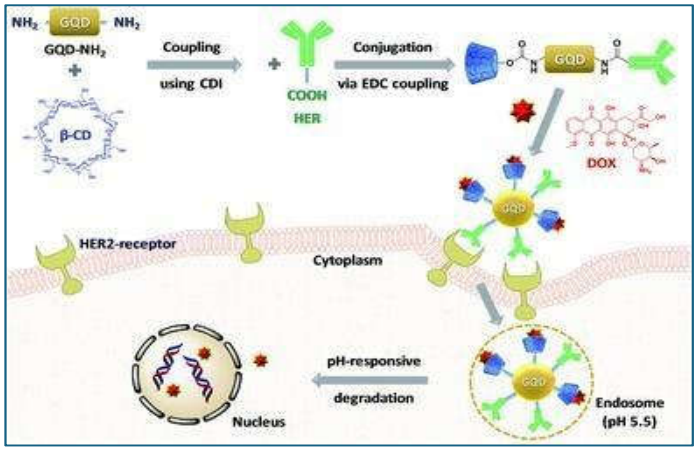

Fig. 1: Schematic illustration of HER-labeled GQD nanocarriers for targeted diagnosis and treatment of HER2-overexpressing breast cancer. Reproduced with permission from Ko, N. R., *et al.* (2017) [13] via RightsLink (License No. 1662701-1). © 2017 royal society of chemistry

Carbon nanomaterials have been at the center stage of nanomedicine and drug delivery, with GQDs gaining recognition because of their distinctive physicochemical characteristics as well as versatility [17]. Since they are extremely small and have huge surface areas, GQDs are able to accommodate ample amounts of drugs. Moreover, their surfaces can be functionalized with unique molecules that help navigate these nanocarriers directly to cancer cells. This results in the drugs releasing precisely where they're required, maximizing efficacy while minimizing damage to healthy tissues. Besides, GQDs possess specific optical properties that allow physicians to visualize tumors in real-time, enabling them to track the progress of treatment [18-21].

The development of such sophisticated nanocarriers in the laboratory may be a slow and expensive process. This explains why computational modeling has turned out to be an effective means of accelerating and facilitating the development process. Density functional theory (DFT) [22] and molecular dynamics (MD) simulations [23] are major techniques that enable the prediction of the behavior of GQDs with drugs and biological systems, determination of their safety, and design optimization, all within a virtual environment. These in silico strategies help simplify the design of smart targeted nanoplatforms to treat difficult cancers such as TNBC [24-26]. This review discusses state-of-the-art computational research to develop GQDS as intelligent, focused tools in breast cancer therapy. To the best of our knowledge, no review study per se deals with computational studies of GQDs as drug delivery or theranostic agents designed specifically toward breast cancer. Although GQD-based therapeutics and experimental progress have been reviewed, in silico research on molecular docking, molecular dynamics and computational design of targeted delivery are under-explored. This gap highlights the need for focused evaluation to advance rational design of GQD nanocarriers for breast cancer theranostics.

Methods

Search strategy

A systematic literature search was conducted to identify research articles focusing on GQD-based drug delivery and theranostic applications for breast cancer treatment. The search was limited to articles published between 2018 and 2025 to capture recent advancements in the field. Established scientific databases, including Scopus, SpringerLink, ScienceDirect (Elsevier), PubMed, and arXiv, were queried using combinations of the following keywords: “graphene quantum dots”, “breast cancer”, “tumor microenvironment”, “targeted drug delivery”, and “theranostics”. From an initial pool of 75 records, 15 articles were selected for detailed review based on their relevance to computational modeling and breast cancer therapeutics.

Inclusion and exclusion criteria

To keep the review tightly focused on in silico–driven insights, studies were selected based on clearly defined inclusion and exclusion criteria. Specifically, the review included research that employed computational modelling approaches such as density functional theory (DFT), molecular dynamics (MD) simulations, or related simulation techniques to explore the properties and behavior of GQDs. Preference was given to studies that examined GQD interactions with breast cancer–relevant biomarkers, anticancer drugs, or components of the TME, as well as investigations highlighting the theranostic potential of GQDs, where therapeutic and imaging capabilities are addressed simultaneously within a breast oncology framework.

Conversely, studies were excluded if they lacked a computational component and were limited to experimental synthesis or physicochemical characterization alone. Research centered on other graphene-based materials, including graphene oxide sheets or carbon nanotubes, was also omitted to maintain specificity toward quantum dots. In addition, broadly framed drug delivery studies that did not directly relate to breast cancer models or mechanisms were not considered, even if they involved nanomaterials. This approach ensured that the final body of literature remained both methodologically consistent and contextually relevant to in silico GQD research in breast cancer.

The challenge: navigating the TME

The complex ecosystem that the cancer cells live in, the TME, is the key to recognizing the challenges of treating breast cancer. Often described by the 'seed and soil' analogy, the cancer cells act as the seeds, while the TME serves as the fertile soil that supports, protects, and nourishes them, providing a favorable environment for growth, progression, and therapy resistance.

The TME is a heterogeneous and dynamic space made of a rich extracellular matrix, blood vessels, and diverse non-cancerous cell types such as immune cells (e. g., T-cells and macrophages) and cancer-associated fibroblasts (CAFs) (fig. 2) [27]. Quite on the contrary, these functional elements are usually used by the cancer to form a pro-tumor immunosuppressive protection. This is especially so in aggressive forms such as TNBC, which

has been known to promote tumor growth and inhibit anti-tumor immunity. Other physical factors like low oxygen (hypoxia) and low pH (acidosis) also increase this protective shield and it is extremely hard to get the conventional drugs to affect and kill the cancer cells.

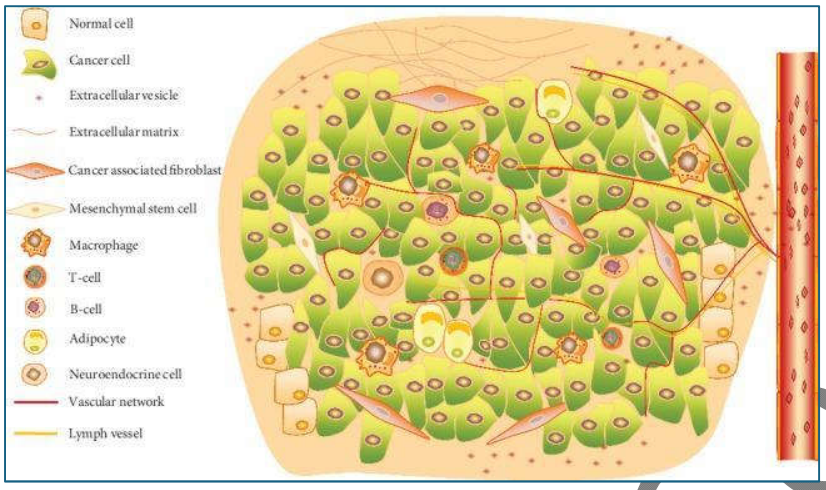

Fig. 2: Schematic illustration of TME depicting its intricate composition of diverse cellular and noncellular components. Copyright © 2020 Rui Wei *et al.* (open access licence: https://creativecommons.org/licenses/by/4.0/)

GQDs: a strategy to navigate the TME

The dense and complex nature of the TME is precisely why nanocarriers like GQDs are so promising. Their unique properties can be engineered to overcome these biological barriers.

Penetrating the "Soil": Due to their incredibly small size (typically<10 nm), GQDs are better equipped to penetrate the dense extracellular matrix and navigate the complex cellular landscape of the TME, reaching cancer cells that larger drug molecules cannot [28, 29].

Targeting Specific Cells: As computational studies have shown, the surface of GQDs can be functionalized with targeting ligands (like folic acid) that seek out and bind specifically to cancer cells, even within a crowded TME. This enables a precision-strike approach so that the therapeutic payload is delivered exclusively to the target [30]. As modelled by Qiu *et al.*, (fig. 3) GQDs can be first chemically conjugated to targeting peptides to recognize cancer cell receptors, while the drug is noncovalently or covalently attached to the GQD surface, creating a single construct that is both targeted and drug loaded [31]. After systemic administration, these functionalized GQDs home in ontumors, bind selectively to overexpressed receptors, and enter cancer cells via receptor-mediated endocytosis. Once internalized, the acidic conditions of endo/lysosomal compartments (pH ≈ 5) promote preferential drug release into the cytoplasm and nucleus.

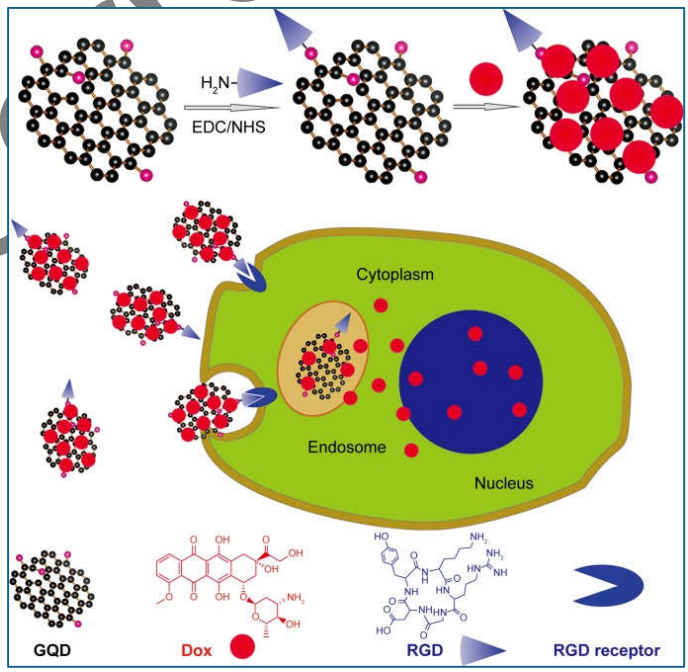

Fig. 3: Schematic of multifunctional GQDs for traceable, targeted anticancer drug delivery and cancer cell interactions. Reproduced from Qiu J *et al.*, © Informa UK Limited (Taylor and Francis). Permission via PLSclear (License Ref No. 110628)

Responding to TME Conditions: GQD-based systems can be designed to be "smart," releasing their drug cargo in response to the specific conditions of the TME. For example, they can be engineered to release drugs in the acidic (low pH) environment characteristic of tumors, ensuring the therapy is activated only where it's needed most [28, 32].

GQDs: a primer for theranostic design

Structure of GQDs

GQDs are sub-10 nm fluorescent fragments of graphene with amazing properties due to their unique structure (fig. 4) [33, 34]. The core of each GQD consists of sp^2-hybridized carbon atoms arranged in a honeycomb configuration, leading to the "quasi-zero-dimensional" nature of GQDs; in other words, the size of GQDs is confined in all three dimensions [35-37]. Unlike an ideal graphene sheet, edges of these dots are decorated with oxygen-containing functional groups including carboxyl (-COOH), hydroxyl (-OH) and epoxy (-O-), which are crucial for making GQDs highly water-soluble and customizable for biomedical applications [38-40]. These functional groups serve as versatile chemical anchors [41]. These anchoring points are important for loading therapeutic drugs by non-covalent p-p stacking, where the aromatic rings of a drug stack onto the GQD core, which is further stabilized by hydrogen bonding [42]. Though less common, covalent bonding of drugs offers a more stable binding, often requiring a specific cleavage mechanism at the tumor site [43]. This functionalization also allows for active targeting of cancer cells. By attaching specific ligands such as folic acid (FA), the GQD can specifically bind to folate receptors that are overexpressed on many TNBC cells, and this tricks the cell into internalizing the nanoparticle in a 'Trojan horse-like' fashion [44]. Ultimately, the ability to combine a high drug payload with precise tumor-targeting capabilities on a single platform is what embodies the full potential of GQDs as next-generation theranostic agents.

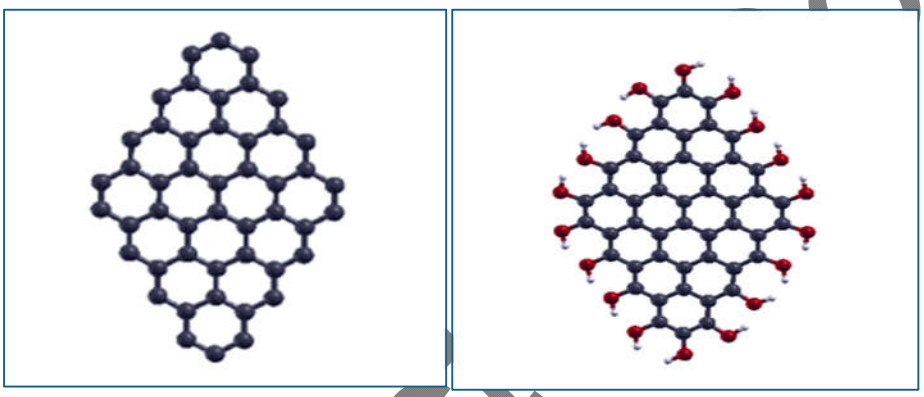

Fig. 4: Optimised structures of GQD (C_{48}) (left) and GQD functionalised by OH radicals ($C_{48}O_{18}H_{18}$) (right) as visualised in 'XCrySDen'

Key properties of GQDs

GQDs have many excellent properties due to their unique structure. Their most important feature is photoluminescence, where GQDs emit intense and stable fluorescence that can be tuned to emit light in different colours by controlling the dot size, shape and surface chemistry. Smaller GQDS typically emit blue colour while and larger dots tending towards green or yellow emission [45-47]. As a type of carbon-based nanomaterials, GQDs exhibit a great biocompatibility and low toxicity, which is partly due to the non-aggregation in biological systems because of hydrophilic edge groups [48-50]. In addition, they possess higher water solubility due to abundant polar functional groups on their surface, which is essential for compatibility with biological fluids [51]. Notwithstanding their very small size, their large surface area permits efficient drug loading [52-54]. Additionally, GQDs have superior photostability as compared to conventional organic dyes or fluorescent proteins and hence are ideal for long term imaging and tracking applications [55-57].

Translation of computational predictions to formulation development

Translating computational predictions into practical pharmaceutical formulations is essential for moving GQD-based nanomedicines from theory to clinic [25]. Computed parameters like adsorption energies and electronic properties describe how GQD-drug complexes will behave. High adsorption energy between doxorubicin and a GQD, for instance, indicates strong binding that minimizes premature drug leakage during storage. A low HOMO-LUMO gap suggests the carrier will respond well to TME triggers such as pH shifts or oxidative stress enabling controlled release at the cancer site. These molecular-level predictions lay the groundwork for formulations that achieve both efficacy and safety. Moving from simulation to actual sterile, stable injectable dispersions involves real challenges in colloidal stability, sterility, and reproducibility. For GQD-based nanomedicines, critical quality attributes (CQAs) including particle size (<50 nm), polydispersity index (PDI<0.30), zeta potential (approximately ±30 mV), drug-loading efficiency, and sterilization stability directly influence therapeutic efficacy and the scope of regulatory approval. MD simulations predict these CQAs by modelling drug-carrier interactions, aggregation dynamics, and surface charge distribution, enabling rational formulation design that reduces experimental iterations. While MD simulations do not directly yield PDI values, they can predict aggregation tendencies and colloidal stability, which in turn affect the experimentally measured PDI. Computationally predicted adsorption energies, zeta potentials, and thermal stability guide drug loading, surfactant/polymer selection for stabilization, and shelf-life optimization, setting rational CQA targets for safe parenteral administration and clinical translation [58]. MD simulations also help anticipate storage-related changes like drug desorption or carrier destabilization allowing formulation scientists to choose appropriate excipients and storage conditions [59, 60].

The formulation process demands precise integration of predicted physicochemical properties with scalable manufacturing constraints and stringent regulatory specifications. Sterilization methods like filtration or heat treatment risk altering the GQD-drug complex's integrity [61]. Polymer coatings such as PEGylation, whose effects on adsorption and release are modeled computationally can enhance stability and shelf life without compromising the responsive release mechanism. These insights help optimize critical parameters such as particle size (ideally<50 nm for deep tumor penetration), polydispersity index, drug loading, and encapsulation efficiency. Ultimately, coupling computational design with formulation development enables the creation of targeted nanomedicines with predictable behavior in vitro and in vivo. By establishing clear links

between computed molecular properties and practical outcomes, colloidal stability, controlled release, and sterile formulations, researchers can accelerate translation from design to clinic [62].

The computational approach: designing GQDs *in silico*

To engineer effective GQD nanocarriers, researchers increasingly turn to computational tools that provide detailed molecular level insights. These in silico methods are useful to predict and understand how GQDs interact with drugs and biological environments, to optimize the loading of drugs into GQD, targeted delivery as well as controlled release before any lab-synthesis [63, 64]. By simulating the entire therapeutic process virtually, computational modeling is accelerating the rational design of smarter, more efficient theranostic agents specifically designed for the treatment of breast cancer.

DFT is a quantum mechanical technique that provides a high-powered "molecular microscope" to understand the basic electronic interactions in a system. In the context of GQD design, DFT is mostly used for calculation of static properties with high accuracy [65-68]. Researchers use it to find out the exact binding energy between the drug molecule and the GQD surface, indicating the strength and nature of the chemical bonds (e. g. π-π stacking, hydrogen bonds) that bind them together [69]. By studying the system's electronic properties, DFT can be used to understand drug adhesion selectivity and how surface modifications of GQDs alter their reactivity, providing insights into optimizing nanocarrier design [70]. The quality of these calculations however relies heavily on the selection of exchange-correlation functional and bases sets. Although hybrid functionalities such as B3LYP are standard, they may not be able to describe long-range dispersive forces that are widespread in graphitic systems. Consequently, the dispersion-corrected functionals (e. g., B3LYP-D3, omegaB97X-D) or the Minnesota meta-hybrid functionals (e. g., M06-2X) are the focus of recent studies to address the aspect of the dispersion-corrected functions necessary to accurately capture the interaction of the pi-pi stacking and van der Waals interaction needed to determine drug adhesion [71-74]. Importantly, the inclusion of dispersion corrections such as D3 or D3BJ is essential for accurately describing π–π stacking and van der Waals interactions dominating GQD–drug binding [75]. Basis-set selection also affects the precision of calculated energies: common choices range from double-zeta basis sets like 6-31G(d) for geometry optimization to extended sets such as 6-311G(d,p) and def2-TZVP, which provide superior accuracy for electronic structure and adsorption energies [76].

If DFT provides us with a static snapshot, MD simulationoffersa long length "molecular film." MD simulations simulate the movement and interaction between atoms and molecules as a function of time using the laws of classical physics [77, 78]. This technique is particularly advantageous in establishing the stability of GQD-drug complex in contact with water molecules and this emulates physiological conditions. Furthermore, MD simulations mimic drug release under environmental stimuli, such as pH shifts replicating acidic TME, enabling observation of unloading kinetics from the GQD carrier. In addition, MD is important to model first contacts between GQDs and cell membranes and can be used to predict how these nanocarriers would approach, adsorb and interact with the cell surface [79, 80]. These simulations depend on proper parameterization of the force field for their reliability. Non-reactive force fields including OPLS-AA [81], CHARMM (C36/CGenFF) and AMBER (GAFF) [82, 83] are commonly used to model conformational changes and non-covalent interactions, whereas reactive force fields (ReaxFF) are used when bond-breaking or bond-formation processes are involved [84]. A critical requirement in these simulations is the accurate treatment of long-range electrostatics using the particle mesh ewald (PME) method, which is particularly important for highly functionalized and charged GQDs [79]. Besides, the standard equilibrium MD does not allow one to observe rare biological events on timescales accessible. Increasingly, therefore, researchers are computing the potentials of mean force (PMF) using enhanced sampling techniques, that is, either umbrella sampling or metadynamics [85]. These methods thusrecreate free energy landscapes that would determine drug desorption under acidic TME conditions or the energy barriers of the GQD penetration of lipid bilayers.

Modelling drug loading and adsorption

Due to their surface chemistry and non-covalent interactions GQDs exhibit high drug retention rates which is supported by DFT and MD simulation analyses. These studies show that the most important mechanisms of drug binding to GQDs are hydrogen bonds and p-p stacking [86]. Sawy *et al.* (2021) [87] showed using DFT studies that DOX is adsorbed to the surface of GQDs (fig. 5) through p-p stack. Further, they fabricated several GQDs and compared them with other types of the carbon materials such as graphene oxide (GO), single-walled carbon nanotubes (SWCNTs) and multi-walled carbon nanotubes (MWCNTs). The study demonstrates that parameters such as particle size, surface charge, cellular uptake, and drug loading capacity critically determine successful drug delivery. Dynamic light scattering (DLS) was used by the team to measure the size and PDI of the particles in order to measure the stability and degree of dispersion of nanocarriers. These tests were conducted before and after loading of DOX in phosphate buffered saline (PBS), pH 7.4 and concentration of DOX, 0.1 mg/ml. Table. 1 gives an overview of the results giving clear understanding of behavior of the nanocarriers in environment resembling the environment of human body. The results showed a marked increase in size after DOX loading, indicating aggregation or thick adsorption layers, which, in turn, could influence cellular uptake.

Table 1: Average particle sizes and polydispersity indexes (PDI) of GQD nanocarriers. Adapted from Sawy *et al.* [87]

Composition	Average size in nm	Dispersity (PDI)
GQD-1	30.14 ± 3.7	0.364 ± 0.21
DOX@GQD-1	99.81 ± 5.3	0.327 ± 0.31
GQDs2	52.7 ± 4.3	0.420 ± 0.19
DOX@GQD-2	107.8 ± 5.7	0.324 ± 0.26
GO	91.99 ± 5.4	0.315 ± 0.032
DOX@GO	179.2 ± 4.1	0.394 ± 0.013
SWCNTs	125.5 ± 1.33	0.362 ± 0.004
DOX@SWCNTs	231.4 ± 4.9	0.342 ± 0.11
MWCNTs	175.6 ± 3.2	0.282 ± 0.009
DOX@MWCNTs	257.63 ± 4.6	0.302 ± 0.215

*PDI-polydispersity indexes, PBS-phosphate-buffered saline, DOX-doxorubicin

Although GO demonstrated the highest DOX loading due to its strong surface charges, this same property can impede timely drug release, thereby reducing therapeutic efficacy. Conversely, smaller GQDs, despite lower loading capacity, demonstrated enhanced drug release and superior anticancer efficacy. This indicates that efficient cellular uptake of DOX is more therapeutically relevant than absolute drug loading levels. This advantage is further highlighted by the poor cellular penetration of larger c-MWCNTs, where size-dependent limitations restrict intracellular delivery and negate therapeutic benefit. The favorable safety profile of GQDs in vivo provides additional evidence for their suitability as drug

carriers, demonstrating that therapeutic efficacy can be achieved without systemic toxicity. Interestingly, stronger DOX-GO binding predictions are in line with the experimental findings of loading (fig. 5) but also point to a significant limitation: strong binding does not ensure a better bioactivity in case it affects the release kinetics. Collectively, such findings establish a critical recommendation in nanomedicine design: therapeutic efficacy is determined not by absolute drug quantity but by the efficiency of nanomaterials in mediating the controlled release and intracellular trafficking.

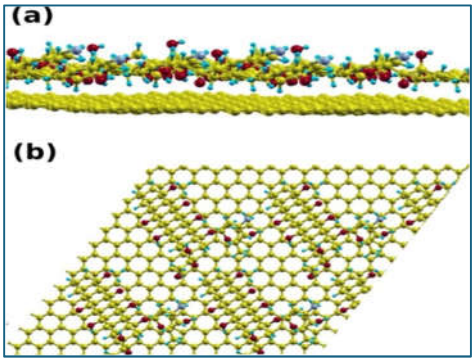

Fig. 5: Optimized structures of (a) DOX on GQD, side view, and (b) DOX on GQD monolayer, top view. Reproduced with permission from Sawy *et al.* (2021) [87] Copyright © [2021], Elsevier via RightsLink (License No. 6130301113860)

In a number of computational investigations, it was shown that surface functionalization of GQDs can greatly improve their drug delivery ability. Interestingly, Vatanparast and Shariatinia (2018) explored the interaction of 5-fluorouracil (5-FU) with pristine and doped GQDs by DFT method. They have found that AlN and AlP doping significantly enhanced the drug adsorption compared to undoped GQDs [88]. Besides improved adsorption, the doping altered the electronic properties of the GQDs which increased interactions with the drug carrier. To be used as effective drug delivery systems, it is necessary to have stable binding between the doped GQDs and 5-FU.

Further, Vatanparast and Shariatinia (2019) went further to study nitrogen-doped GQDs (N-GQDs) and showed that the electronic and structural properties may be tuned by a controlled nitrogen doping process [89]. By combining DFT calculations and MD simulations, they found that nitrogen doping greatly strengthens drug-nanocarrier interactions and provides the ability to control drug release. Among the nitrogen species analyzed (graphitic, pyridinic, and amide), graphitic nitrogen sites located at the GQD center showed the strongest binding affinity for gemcitabine compared with pristine and edge doped GQDs. The adsorption process was controlled mainly by van der Waals interactions and was thermodynamically favorable (negative ΔG values). These results were also confirmed by quantum theory of atoms in molecules (QTAIM) and noncovalent interaction index (NCI) calculations.

MD simulations showed that, although all nanocarriers were able to load the drug, controlled release was most efficient under acidic conditions (mimicking the TME). Steered molecular dynamics further demonstrated that N-GQDs with a perpendicular orientation of drug loading showed improved membrane penetration suggesting enhanced cellular uptake. Taken together, these results render center-doped N-GQDs as promising cancer drug carriers with excellent binding and pH-responsive release properties for cancer treatment.

More recently Munny *et al.* (2023) applied DFT to investigate the adsorption of cisplatin (CPT) on pristine and differentially doped GQDs [90]. It is shown that boron-doped GQDs (B-GQDs) have the highest binding affinity and highest electron transfer capacity and thus are the best candidates for CPT delivery. The adsorption energies of B-GQDs in gas and solvent phase were significantly higher, along with significant electron transfer between CPT and the nanocarrier. This electron transfers greatly reduced the electronic band gap (E_g) for improved electrical conductivity with the potential to boost the responsiveness to drug binding and release. The increased sensitivity of B-GQDs to CPT is further manifested in the increased global softness, characterizing a favorable interaction. Taken together, this study demonstrates the superior drug binding properties provided by boron doping and makes B-GQDs promising for future experimental nanomedicine applications [90]. A comparative study of adsorption energies, free energy and enthalpy changes among these GQD nanocarriers is represented in table 2 [87-90].

Table 2: Comparison of adsorption or binding energies, enthalpy changes and Gibbs free energy for various GQD structures interacting with anticancer drugs, highlighting differences in interaction strength and thermodynamic stability

GQD structure	Drug loaded	Adsorption energy (E_{Ad})/Binding energy (E_b) kcal/mol	ΔH_{ad} kcal/mol	ΔG_{ad} kcal/mol	Ref.
DOX@GQDs	Doxorubicin	-40.36	-	-	Savy *et al.* 2021 [87]
GQD BN-FU1	5-Fluorouracil	-17.36	-15.41	-5.14	Vatanparast, 2018
GQD BP-FU1	5-Fluorouracil	-21.65	-20.24	-8.26	[88]
GQD AlN-FU1	5-Fluorouracil	-47.29	-45.90	-32.50	
GQD AlP-FU1	5-Fluorouracil	-30.61	-29.26	-17.62	
Pristine GQD	Gemcitabine (GC)	-11.94	-16.68	-0.53	Vatanparast, 2018
GQD+pyrazole	Gemcitabine (GC)	-11.84	-17.19	-0.97	[89]
GQD+pyridazine	Gemcitabine (GC)	-12.27	-17.31	-1.35	
GQD+graphite @ centre	Gemcitabine (GC)	-13.92	-20.32	-3.68	
GQD+pyridine @ centre	Gemcitabine (GC)	-15.32	-22.66	-6.68	
GQD+pyridine @ edge	Gemcitabine (GC)	-12.12	-17.26	-1.12	
GQD+amido @ centre	Gemcitabine (GC)	-13.71	-20.01	-3.25	
GQD+amido @ edge	Gemcitabine (GC)	-11.77	-15.14	-0.43	
CPT-BN/Gra QD (gas media)	Cisplatin (CPT)	-20.29	-	-8.26	Munni *et al.* 2023
CPT-B/Gra QD (gas media)	Cisplatin (CPT)	-33.21	-	-7.47	[90]

CPT-N/Gra QD (gas media)	Cisplatin (CPT)	-23.75	-	-8.68

**Adsorption energies listed for Doxorubicin, 5-Fluorouracil, and Cisplatin represent the energy change upon drug adsorption on nanocarriers. For Gemcitabine, the values denote binding energies calculated in a similar manner. E_{Ad}, E_b, ΔH_{ad} andΔG_{ad} inkcal/mol. More negative E_{Ad}/E_b values correspond to stronger interactions between the GQD and the adsorbed molecule.

Although the literature unanimously confirms the effectiveness of surface functionalization and doping in improving drug payload, a direct quantitative comparison of adsorption energy between these studies is difficult because of the heterogeneity of methods. This change in reported binding affinities is not only due to the type of dopant (e. g., B, N, Al) or drug molecule, but also depends on a variety of computational configurations (e. g., B3LYP vs. M06-2X), basis sets, and the choice of solvation models (gas phase vs. implicit/explicit solvent). These inconsistencies complicate the concept a universal structure-affinity relation to GQD design. Moreover, a critical knowledge gap exists regarding the "Goldilocks zone" of optimal binding strength, as seen with GO where maximizing adsorption energy via doping unintentionally suppresses drug release rates, causing payload retention. The future in silico research should thus go beyond the calculation of statical binding energies and standardized benchmarking protocols that will emphasize on the reversibility of binding under tumor conditions (pH, temperature) to gain an accurate insight into the prediction of therapeutic bioavailability.

Controlled drug release-simulation

A smart nanocarrier should not merely be a secure carrier of its load but also be able to release its cargo whenever required at the desired location. MD simulations are known to model these dynamic processes effectively. Apparently, a healthy tissue has a pH of 7.4, whereas the tumor microenvironment has a relatively lower pH of around 6.5 often stimulating the drug release naturally [91]. MD simulations are equipped toprovide a more atomistic perspective of drug release whenGQDs are surface-modified with co-polymers (PEG-b-PLA) as shown by Yoosefianand team [77]. The researchers used the GROMACS package and CHARMM36 force field in this work to model the interaction of docetaxel (DTX) with bare and copolymer-coated GQDs in a liquid medium. PEG-b-PLA copolymer was incorporated to enhance solubility and change the dynamics of drug release.

The findings showed that DTX was adsorbed rapidly and consistently to the GQD surface even without copolymer modification. One factor that is extremely important in controlling drug release is steric hindrance that led to the initial delay in drug adsorption when the nanocarrier was coated with PEG-b-PLA. The penetration of the copolymer layer by DTX, followed by the formation of steady interactions between the GQD and DTX during the simulation, resulted in a pattern of delayed yet sustained adsorption. Advanced energy profiling and contact tracking techniques demonstrated improved drug solubility and release properties and validated that the copolymer is instrumental in designing nanocarrier strategies to achieve targeted chemotherapy. The essential variations in the adsorption and release performance of the bare and PEG-b-PLA-modified graphene quantum dots, as shown by the MD simulations, are listed in table. 3, which demonstrates the modulatory influence of copolymer surface modification on adsorption kinetics, stability, solubility, and controlled release behavior.

Table 3: Comparative analysis of MD simulation outcomes illustrating DTX adsorption and release behavior on bare GQD versus PEG-b-PLA surface-modified GQD

Parameter	Bare GQD+Docetaxel	PEG-b-PLA-Modified GQD+Docetaxel
Simulation time analyzed (ns)	50	50
Average number of drug–carrier contacts	~30 contacts (stable after ~10 ns)	~15 contacts initially, rising to ~28 after 40 ns
Lennard-Jones interaction energy (kJ/mol)	~-120 to-130 (stable)	~-100 initially, stabilizes near-125
RMSD for DTX (nm)	~0.2 nm (stable binding)	~0.25 nm (initial fluctuations, stabilizes later)
Radial distribution function (Peak distance, nm)	~0.35 nm (close contact)	Initial peak at ~0.5 nm (polymer barrier), shifts to ~0.35 nm
Solvent accessible surface area (SASA) (nm^2)	Lower (less exposed)	Higher SASA due to polymer coating

Adapted from Yoosefian *et al.* [77]

Although copolymer modification (PEG-b-PLA) effectively enhances solubility and enables sustained release, these simulations reveal a fundamental trade-off: the same steric barrier that prolongs release also hinders the initial drug loading process. This permeability-retention conflict can be lost at shorter MD simulations, and this issue might not be fully reflected by the long-term stability of the polymer coating under physiological shear forces. Moreover, while pH-responsiveness is frequently cited as a release trigger, most standard MD studies-including this one-model pH effects implicitly by fixing protonation states, rather than simulating dynamic proton exchange. To truly predict in vivo efficacy, future computational models must integrate these polymer dynamics with explicit pH-titration methods, rigorously testing whether the 'sustained release' observed over nanoseconds translates to the days-long stability required for clinical translation.

Computational clues to the GQD-based diagnostics (The "theranostic" aspect)

The real promise of the GQDs in cancer therapy is achieved when the diagnostic and therapeutic properties of GQDs are combined in one, "theranostic" platform. Computational studies are crucial to the design of these all-in-one systems, especially for predicting their imaging properties and modeling their complex behaviour in the biological environment [92].

GQD's photoluminescence (PL), which is intrinsic and allows them to be used as fluorescent probes for bioimaging, is their most attractive diagnostic feature. The understanding and prediction of these optical properties necessitates the employment of computational methods, particularly time-dependent density functional theory (TD-DFT).

Researchers have predicted the wavelength of fluorescence emission of a GQD via TD-DFT simulations to calculate the electronic excited states. The high tunable nature of the PL of GQDs has been confirmed by using these models [93]. For instance, in a study published by Drissi *et al.* in 2020, TD-DFT was used to show that introducing edge functional groups such as-OH and-COOH to GQDs redshifts their optical transitions, which is considered to be more suitable for near-infrared bioimaging applications [94].

Work by Nhan *et al.* in 2018 also showed that both the size and the edge groups have a direct influence on the color emission of the GQDs, a process that has been attributed to quantum confinement and edge state [95]. Furthermore, simulations can be used to predict the change in the fluorescence of the GQD on loading drugs. Elkabiri *et al.* (2025) have performed an exhaustive theoretical analysis of GQDs covalently linked with the anticancer drug DOX. Their TD-DFT calculations revealed these GQD-DOX hybrids exhibit high near-infrared photoluminescence making them

highly suitable for bioimaging and drug delivery simultaneously. The research showed that by varying both the drug loading and the type of chemical linkage such as C-C, C-O or C-N bonds, the electronic and optical properties of these systems can be tuned very significantly (fig. 6).

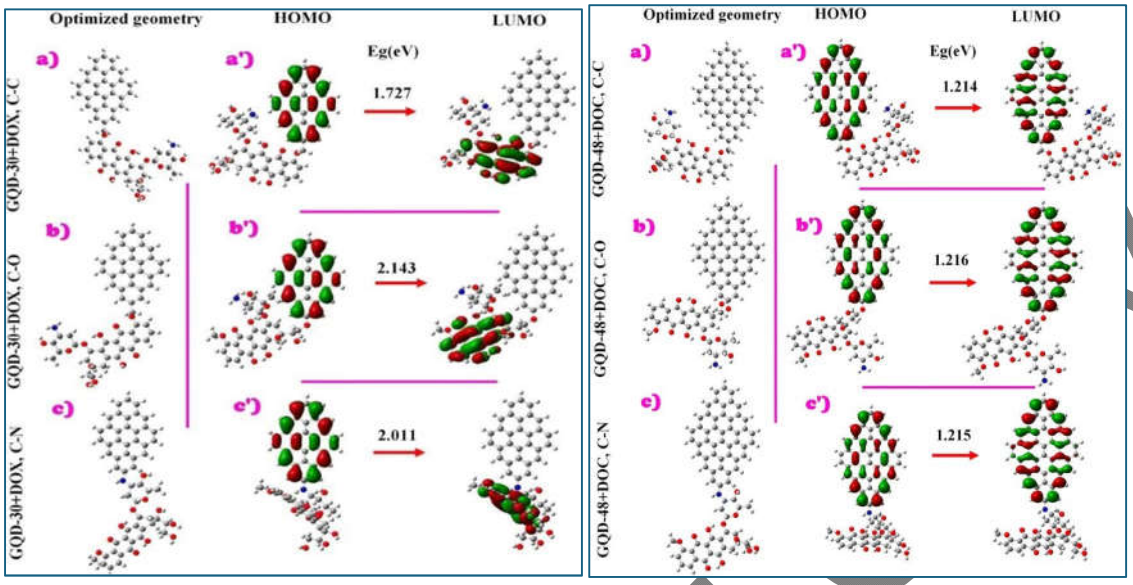

Fig. 6: Schematic representations of the molecular structures of the six studied (GQD+DOX) configurations at different loading states: DOX-30 (left) and DOX-48 (right). For each system, three bonding types C–C, C–O, and C–Nare shown (panels a–c). Corresponding frontier molecular orbital plots (panels a′–c′) illustrate the HOMO and LUMO distributions and energy gaps for each configuration [96]. Copyright © Royal Society of Chemistry. Reproduced with permission of the RSC Publishing through CCC, License No. 1662712-1

As the GQD size and its conjugation to DOX grows, there is a clear trend of decreasing HOMO-LUMO energy gap. This trend is expected to enhance photoluminescence and drive a redshift in absorption, both of which are critical for effective imaging and therapeutic tracking. The spatial distributions of HOMO and LUMO orbitals are sensitive to the nature of the linkage, suggesting that interfacial chemistry is critical in determining charge transfer and the behavior of nanocarriers. Altogether, this computational insight highlights how accurate molecular engineering at the GQD-drug interface allows the rational design of nanocarriers with tunable properties putting forward a route to more effective drug delivery and advanced theranostic applications [96]. In an extended study [97], the same authors demonstrated a decrease in the HOMO-LUMO energy gap in response to functionalization with MTX that depended on the size of the GQD and the type of bonding, but the intrinsic optical properties of the GQDs were found to be barely affected. Larger GQDs maintained a stable near-infrared absorption and photoluminescence, which is suitable for deep tissue imaging, and smaller dots exhibited a shift in the emission from visible to near-infrared. Importantly, the $C_{48}H_{18}$ GQD with a C-O bond showed the best photoluminescence performance with a high oscillator strength and minimal spectral line width and thus appears to be a particularly good candidate for cancer imaging and therapy. As could be seen in the Tables. 4 and 5 the optical properties can be accurately compared between different GQD structures and sizes.

Table 4: Comparative electronic properties and derived global reactivity descriptors of various GQD structures

GQD structure	$E_{HOMO\ (eV)}$	$E_{LUMO\ (eV)}$	$E_{g\ (eV)}$	μ	η	ω	Ref
GQD BN-FU1	-5.62	-1.61	4.02	-3.62	2.01	3.26	Vatanparast, 2018 [88]
GQD BP-FU1	-5.72	-2.17	3.55	-3.94	1.77	4.38	
GQD AlN-FU1	-4.83	-2.75	2.08	-3.79	1.04	6.91	
GQD AlP-FU1	-5.48	-2.35	3.13	-3.91	1.57	4.88	
Pristine GQD+GC	-6.17	-1.83	4.34	-4.00	2.17	3.69	Vatanparast, 2018 [89]
Pyrazole N-doped GQD+GC	-5.51	-2.68	2.82	-4.09	1.41	5.94	
Amido at edge N-doped GQD+GC	-5.86	-1.74	4.12	-3.80	2.06	3.50	
CPT-BN/Gra QD (gas media)	-4.58	-3.55	1.03	-4.07	0.52	16.04	Munni *et al.* 2023 [90]
CPT-B/Gra QD (gas media)	-5.10	-4.87	0.23	-4.99	0.12	106.2	
CPT-N/Gra QD(gas media)	-3.66	-3.28	0.38	-3.47	0.19	32.16	
$C_{30}H_{14}$+DOX	-4.4	-2.68	1.727	-3.542	0.863	14.53	Elkabiri *et al.* 2025 [96]
$C_{48}H_{18}$+DOX	-4.0	-2.8	1.214	-3.405	0.607	19.1	
$C_{30}H_{14}$+MTX (CC bond)	-4.581	-2.392	2.189	-3.486	1.094	11.1061	Elkabiri *et al.* 2025 [97]
$C_{30}H_{14}$+MTX (CO bond)	-4.677	-2.483	2.194	-3.58	1.097	11.6831	
$C_{30}H_{14}$+MTX (CN bond)	-4.764	-2.574	2.19	-3.669	1.095	12.2936	
$C_{48}H_{18}$+MTX (CC bond)	-4.289	-3.078	1.211	-3.683	0.605	22.4082	
$C_{48}H_{18}$+MTX (CO bond)	-4.221	-3.002	1.219	-3.611	0.609	21.3993	
C48H18+MTX (CN bond)	-4.311	-3.096	1.215	-3.703	0.607	22.5776	
PEI N-doped GQDs	-5.00	-2.99	2.01	1.01	-	8.02	Gunes *et al.* [108]
PdNPs/PEI N-doped GQDs	-4.15	-2.98	1.17	0.59	-	3.72	

*E_g – band gap energy, μ-chemical potential, η-hardness, ω-electrophilicity index

Table 5: Comparative study of E_{abs}, E_{em}, λ_{abs}, λ_{em} and the stokes shift of various GQD structures

GQD structure	E_{abs}	λ_{abs}	E_{em}	λ_{em}	Stokes shift (eV)	Ref
$C_{30}H_{14}$-H	2.334	531.20	2.179	568.9	0.155	Drissi *et al.*
$C_{30}H_{14}$-CH_3	2.190	566.10	2.038	608.2	0.152	2020 [94]
$C_{30}H_{14}$-OH	2.223	557.70	2.081	595.8	0.142	
$C_{30}H_{14}$-COOH	1.996	621.30	1.657	748.1	0.339	
$C_{30}H_{14}$	2.345	528.72	2.1984	590.75	0.147	Elkabiri *et al.*
$C_{48}H_{18}$	1.446	857.299	1.289	954.639	0.157	2025 [96]
$C_{30}H_{14}$+DOX	1.287	963.5	0.68	1808	0.685	
$C_{48}H_{18}$+DOX	1.092	1136	1.03	1199	0.059	
$C_{30}H_{14}$+MTX (C–C bond)	1.97	629.1	0.549	2258.7	1.421	Elkabiri *et al.*
$C_{30}H_{14}$+MTX (C–O bond)	2.238	553.9	1.418	874.25	0.82	2025 [97]
$C_{30}H_{14}$+MTX (C–N bond)	1.65	751.5	0.458	2708.7	1.192	
$C_{48}H_{18}$+MTX (C–C bond)	1.595	777.7	0.855	1451.7	0.74	
$C_{48}H_{18}$+MTX (C–O bond)	2.25	551.1	1.607	771.65	0.642	
$C_{48}H_{18}$+MTX (C–N bond)	1.231	1006.8	0.393	3154.6	0.848	

E_{abs} = absorption energy in eV, E_{em} = emission energy in eV, λ_{abs} = absorption wavelength in nm, λ_{em} = emission wavelength in nm

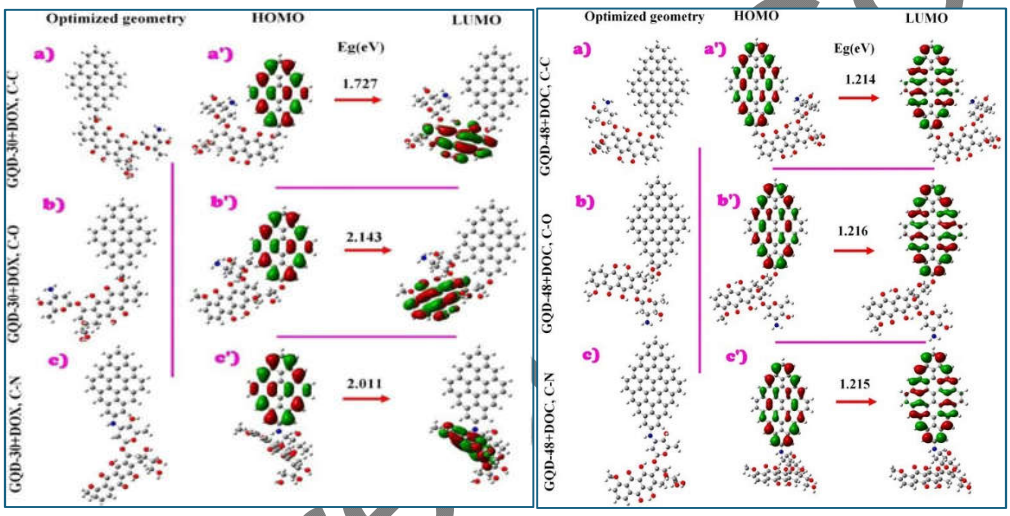

Fig. 6: Schematic representations of the molecular structures of the six studied (GQD+DOX) configurations at different loading states: DOX-30 (left) and DOX-48 (right). For each system, three bonding types C–C, C–O, and C–Nare shown (panels a–c). Corresponding frontier molecular orbital plots (panels a′–c′) illustrate the HOMO and LUMO distributions and energy gaps for each configuration [96].

When considering GQDs for drug delivery, their electronic properties are not merely theoretical parameters but directly determine how effectively these nanocarriers perform in physiological environments. For instance, the gap between HOMO and LUMO energy levels (E_g) tells us about how easily the quantum dot participates in chemical interactions [98]. Doping GQDs tends to lower E_g, boosting their reactivity and, as recent studies suggest, making it easier for these carriers to interact with cell membranes [99]. This simple shift could improve how drugs enter cells and enhance the overall therapeutic outcome which is crucial when designing drug delivery systems. Beyond the band gap, other factors like electrophilicity (ω) help us predict how strongly a GQD can hold onto drugs, while hardness (η) relates to stability during circulation in the body [100]. Our data show that GQDs with higher ω values often grab and hold drug molecules more effectively, and the ones with optimal hardness maintain integrity until they reach their target. The emission and absorption properties also matter. If a GQD emits in the near-infrared range, for example, that can allow us to track drug delivery deep in tissue using imaging techniques [101]. Meanwhile, a larger Stokes shift means clearer signals for monitoring payload movement, which is extremely helpful for theranostics, where therapy and diagnosis are combined [102].

Although computational studies have demonstrated the tunability of GQD optical properties via functionalization and doping, a critical review of the literature reveals significant inconsistencies that hinder direct comparison across studies. The HOMO-LUMO gaps and emission wavelengths reported tend to differ dramatically even between similar GQD structures, which in part is caused by the variety of computational methods used, and not the specific characteristics of the materials. In particular, the exchange-correlation functional selection (e. g., B3LYP vs. CAM-B3LYP vs. PBE) and basis sets have a significant influence on the precision of excited-state calculations (TD-DFT). Moreover, most studies model such transitions in the gas phase or implicit solvation models (PCM), and do not take explicit solvent interactions or local pH effects, which are known to quench or shift fluorescence in biological systems into account. Therefore, it is not yet possible to design an effective, universal guideline on the definition of the concept of NIR-active GQDs. The way forward in future studies needs to be standardized benchmarking of the functionals with experimental optical measurements, and the inclusion of explicit solvation dynamics to close the disconnect between theory and practice in bioimaging.

Biocompatibility and cellular interactions

For any GQD-based platform to be clinically viable, it will have to be both safe and effective. Computational studies are not only important to predict the safety and possible toxicity of new GQD designs, but also important to understand how these designs affect the cell processes that result in a therapeutic response such as cancer cell death [103].

Predicting safety and genotoxicity

A critical issue of any nanomedicine is the possibility of causing unintended damage to the genetic material (genotoxicity). In silico models have played a key role in the exploration of these risks and the creation of design rules for safer GQDs.

MD simulations by Kong *et al.* [104] and Liang *et al.* [105] have uncovered that DNA damage due to GQD is often size dependant which can be greatly mitigated by rational design of the particle size and surface chemistry. Kong's research paper examined the interaction of GQDs of different sizes (GQD7, GQD19, GQD61, and GQD275) and DNA and showed fundamentally different damage mechanisms depending upon particle dimensions. As illustrated in fig. 7, smaller sized GQDs (GQD7) preferentially intercalate between base pairs, and therefore cause localized structural distortions, while larger sized GQDs (GQD61) adsorb at the DNA ends and cause severe unwinding of the DNA helix.

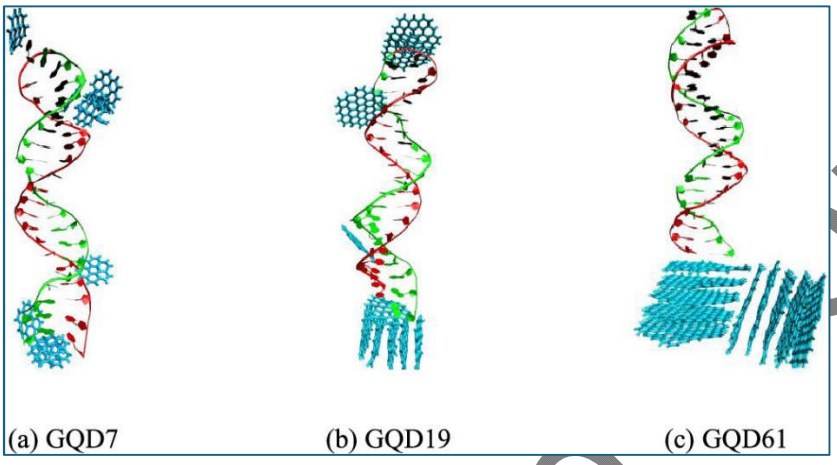

Fig. 7: MD snapshots illustrating the size-dependent genotoxicity of GQDs on double-stranded DNA. (a) Small GQDs (GQD7) tend to intercalate into the helix, disrupting base pairing. (b) Medium GQDs (GQD19) exhibit intermediate binding. (c) Large GQDs (GQD61) act as a surface platform, inducing terminal adsorption and significant unwinding of the DNA helix. Adapted with permission from Kong, Z. *et al.*, J. Phys. Chem. B 2020, 124(42), 9335–9342. Copyright 2020 American chemical society

Building on the size-dependent toxicity observed in Fig.7, MD simulations further reveal that the specific genetic sequence plays a critical role in how quickly DNA is damaged by large nanocarriers. As illustrated in fig. 8, the interaction dynamics of large GQDs (GQD61) differ significantly between G-C rich and A-T rich strands over time.

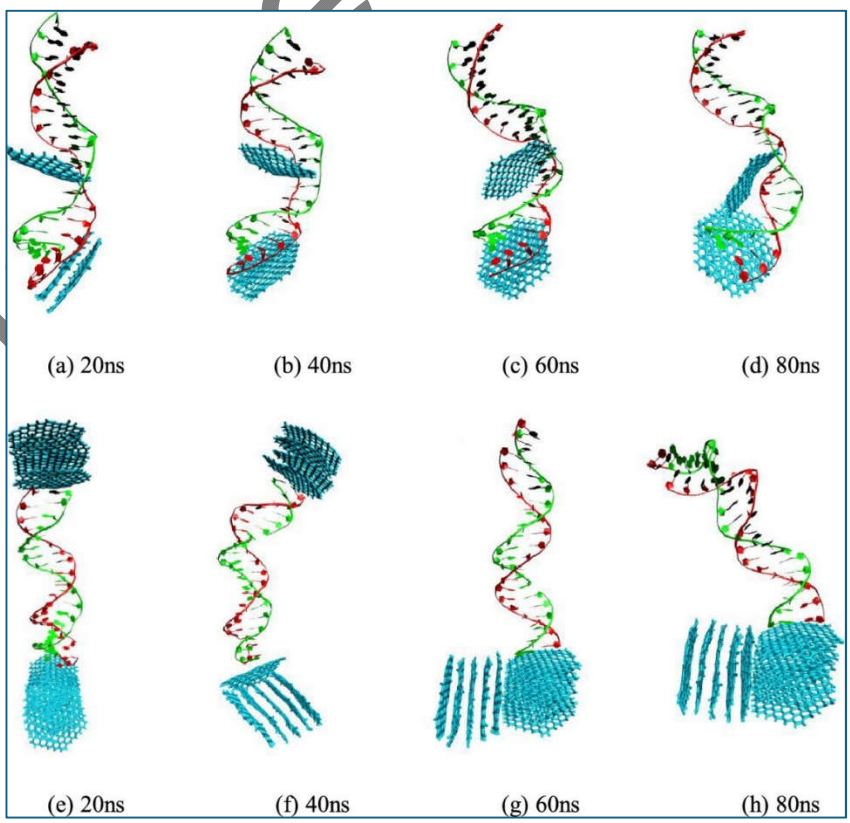

Fig. 8: MD snapshots (20–80 ns) showing the sequence-dependent structural stability of DNA upon interaction with GQD61, with enhanced terminal unwinding observed in the A–T rich sequence (top row) compared to the G–C rich sequence (bottom row). Adapted with permission from Kong, Z. *et al.*, *J. Phys. Chem. B* 2020, *124*(42), 9335–9342. Copyright 2020 American chemical society

Liang *et al.* demonstrated the selective adsorption behavior of several DNA sequences on GQDs. According to the study, stronger pi-pi stacking interactions cause guanine-rich sequences (poly G) to adsorb more firmly and steadily than cytosine-rich sequences (poly C) (fig. 9).

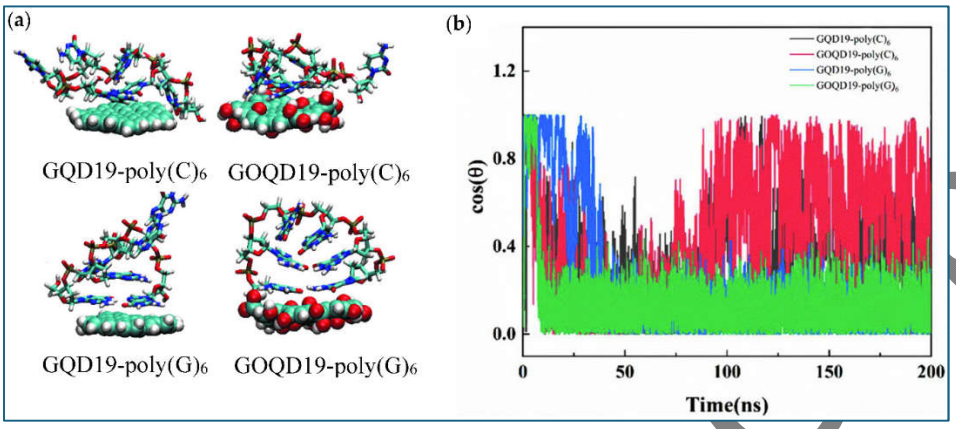

Fig. 9: Molecular dynamics snapshots and orientation analysis illustrating the adsorption behavior of single-stranded DNA oligonucleotides (poly(C)$_6$ and poly(G)$_6$)on pristine (GQD19) and oxidized (GOQD19) graphene quantum dots. Reproduced from Liang, L. *et al.*, Materials 2022, 15(21), 7435, under CC BY 4.0 license

Surface oxidation of graphene quantum dots (GQDs) has become one of the most promising methods to suppress genotoxicity, which essentially obstructs size-dependent damage effects. Although the bigger pristine GQDs tend to cause severe structural unwinding of DNA, Liang *et al.* (2022) showed that oxygen-functionalized GQDs (GOQDs) have an extraordinary protecting impact when used (fig. 10).

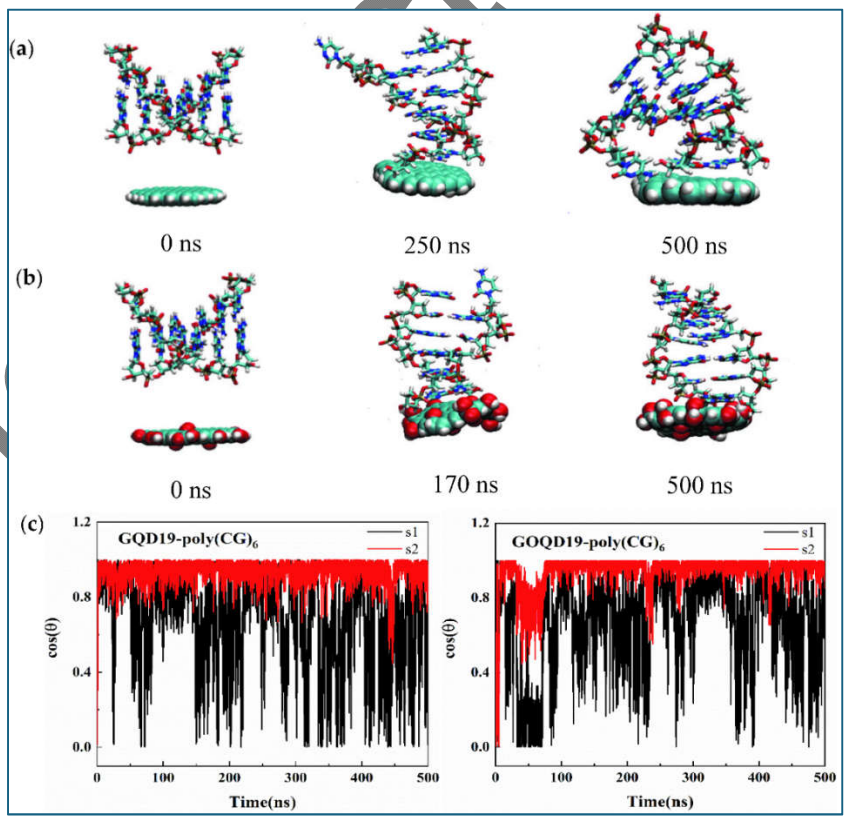

Fig. 10: MD simulation snapshots compare the adsorption of double-stranded DNA on (a) pristine GQD19 and (b) oxidized GOQD19. While the pristine surface causes significant unwinding and structural collapse, the oxidized surface preserves the DNA's double-helix structure by inducing a stable vertical adsorption orientation. (c) Orientation angle analysis cos(θ) confirms the stability of the DNA on the oxidized surface over 500 ns. Reproduced from Liang, L. *et al.*, Materials 2022, 15(21), 7435, under CC BY 4.0 license

This decrease in toxicity is guided by a significant decrease in binding affinity of the nucleobases for the nanocarrier surface. DFT calculations by Kong *et al.* (2020) showed that carboxyl and hydroxyl functionalization decreased the binding energy to the DNA bases as compared to plain surfaces by about 30-50%. The working principle is based on the electrostatic repulsive interaction of the negatively charged functional groups on GOQD surface and phosphate backbone of DNA. This protective mechanism relies on electrostatic repulsion between the negatively charged functional groups on the GOQD surface and the DNA phosphate backbone. This repulsion maintains physical separation between the molecules, preventing the intimate pi-pi stacking interactions responsible for base damage. Consequently, surface chemistry is a primary determinant of biosafety: large, oxidized GQDs cause substantially less structural damage than even small, pristine GQDs [105].

These computational understanding creates a clear actionable roadmap for designing safer GQD-based therapeutics. The combined results of the two studies provide the concrete design guidelines for safer GQDs summarized in table 6.

Table 6: Key physicochemical parameters of GQDs optimized for reduced genotoxicity in biomedical applications. Adapted from Kong *et al.* [104] and Liang *et al.* [105]

Parameter	Optimal range for reduced genotoxicity	Rationale
Size	<5 nm diameter (GQD7–GQD19)	Minimizes DNA unwinding and structural disruption
Oxidation level	Moderate (C/O ratio 2–4)	Balances water dispersibility with reduced DNA binding
Functional groups	–OH and –COOH preferred	Provide electrostatic repulsion and enhance hydrophilicity
Concentration	<10 µg/ml for biomedical use	Prevents cooperative aggregation effects

In addition, researchers have shown that through a combination of moderate oxidation and ultra small particle size, GQDs can be effectively "pacified" and their genotoxic potential significantly reduced without compromising drug delivery functionality. The convergent results in several independent computational studies strongly support the principle that GQD genotoxicity is not a fixed property but one that is designable-i. e., one can be engineered away through strategic surface modification. This mechanistic understanding will help speed the translation of GQD theranostics into clinical applications, especially for cancer therapies in which reducing off-target genomic damage is of crucial importance to therapeutic safety.

Understanding the mechanisms of biology

Beyond safety, computational design can be directly related to therapeutic efficacy. The chemical properties of a GQD, which can be modeled and optimized in silico, have a direct impact on how it interacts with cancer cells and initiates certain biological responses [106]. For instance, a study by Ku *et al.* (2023) showed experimentally that the extent of oxidation on the surface of a GQD plays an important role in its anticancer activity. Highly oxidized GQDs cause high level of intracellular reactive oxygen species (ROS), and this leads to activation of signaling pathways such as p38 (mitogen-activated kinase) and p53/p21, and activation of these signaling pathways leads to apoptosis and cell cycle arrest in breast cancer cells (fig. 11) [107].

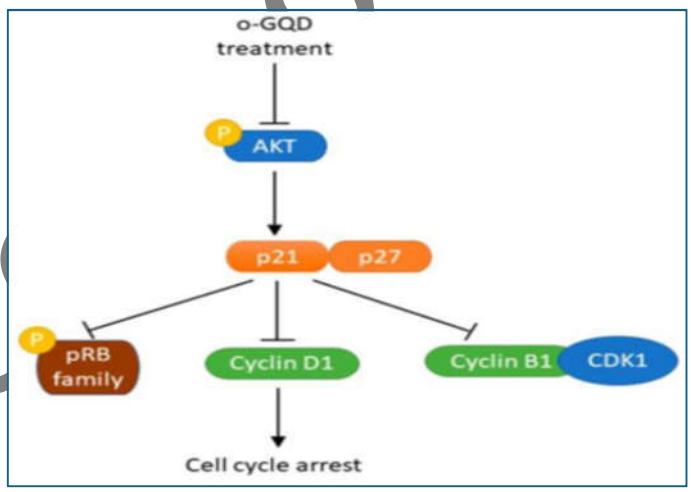

Fig. 11: Illustration of the signalling pathways modulated by o-GQDs in breast cancer cells, leading to cell cycle arrest and apoptotic cell death. Reproduced with permission from Ku *et al.*, (2023). Published under CC BY 4.0 license [107]

Similarly, Gunes *et al.* (2024) employed a combined experimental and computational approach to investigate how palladium nanoparticle (PdNP) decoration enhances the anti-ovarian cancer activity of nitrogen-doped GQDs (PEI N-GQDs) [108]. First, the modification significantly narrowed the HOMO–LUMO energy gap-dropping from 2.01 eV in the pristine N-GQD to 1.17 eV in the PdNP-decorated composite (table 7), providing a direct quantitative indicator of increased chemical reactivity and electron-donating capability.

Table 7: Comparative electronic, thermal, and frontier molecular orbital properties of PEI N-doped GQDs and PdNPs/PEI N-doped GQDs nanocomposites in water at 298.15 K

Property	PEI N-doped GQDs	PdNPs/PEI N-doped GQDs
Dipole (Debye)	6.92	6.62

Polarizability (a. u.)	733.53	800.84
Thermal Energy (eV)	897.62	898.63
Heat Capacity (cal/mol K)	306.14	310.23
Entropy (cal/mol K)	443.19	460.78
HOMO (eV)	-5	-4.15
LUMO (eV)	-2.99	-2.98
ΔE (HOMO–LUMO gap, eV)	2.01	1.17
Ionization Potential (eV)	5	4.15
Electron Affinity (eV)	2.99	2.98
Hardness η (eV)	1.01	0.59
Electronegativity χ (eV)	4	3.57
Electrophilicity ω (eV)	8.02	3.72
Softness σ (1/eV)	1	1.71

Adapted from Gunes *et al.* (2024) [108]

This heightened reactivity was further mapped through molecular electrostatic potential (MEP) isosurfaces, which revealed distinct zones of charge separation at the PdNP interface, creating active sites primed for electrophilic and nucleophilic attacks. Concurrently, density of states (DOS) plots showed a proliferation of new electronic states near the Fermi level (fig. 12), confirming that the metal-decoration introduced specific catalytic centers absent in the bare GQD. These electronic features were not merely theoretical. Intermolecular interaction mapping (IGM) pinpointed strong, non-covalent interaction regions that facilitate binding with cellular membranes. Experimentally, these specific electronic alterations translated into a superior biological phenotype: the PdNP-functionalized GQDs exhibited significantly higher efficacy in inducing cell cycle arrest and apoptosis compared to their non-functionalized counterparts. By linking the computed drop in the band gap to the observed increase in cytotoxicity, this study demonstrates how regulating the electronic structure of a nanocarrier can directly tune its therapeutic potency.

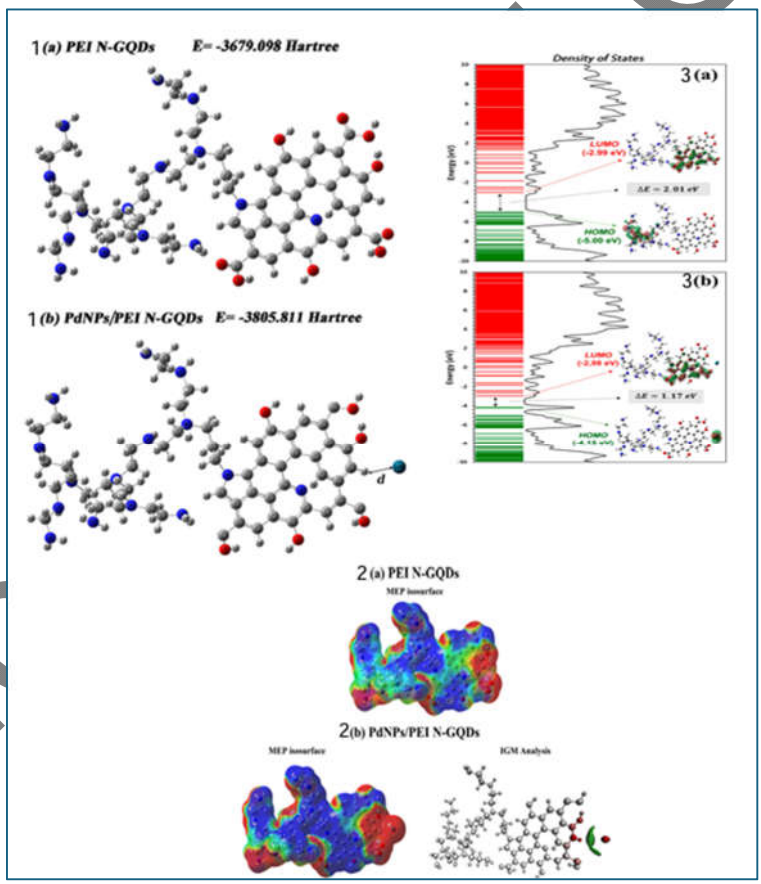

Fig. 12: DFT-optimized molecular structures of PEI N-GQDs [1(a)] and PdNPs/PEI N-GQDs [1(b)], with respective total energies provided. MEP isosurfaces of PEI N-GQDs [2(a)] and PdNPs/PEI N-GQDs [2(b)], illustrating changes in charge distribution upon Pd nanoparticle decoration. DOS plots for PEI N-GQDs [3(a)] and PdNPs/PEI N-GQDs [3(b)], showing the narrowing of the HOMO-LUMO gap with Pd decoration. Insets depict corresponding frontier molecular orbitals with energy values. Reproduced from Gunes *et al.* [108]. Copyright © 2024 the authors. Published by the American Chemical Society. Licensed under CC-BY 4.0

Challenges and hurdles in pharmaceutical development and translation

While computational models have significantly advanced the design of GQD theranostic agents, a substantial gap remains between theoretical prediction and clinical translation. A primary challenge lies in bridging the idealconditions of in silico models with the stochastic, dynamic reality of

biological systems [109]. Current simulations often simplify physiological interactions, whereas the in vivo environment is characterized by a vast heterogeneity of cell types, protein coronas, and fluctuating hemodynamic conditions.

To ensure that the projected efficiency of targeting, controlled drug release, and compatibility with biological systems are consistently and accurately predicted in living environments, it is necessary to establish a closer integration between computational forecasts and experimental evaluations [110]. Some critical challenges specific to pharmaceutical development and translation are given below.

Protein corona formation and its impact on GQD theranostics: A significant obstacle in this context is the realistic modeling of the protein corona which develops upon the introduction of nanoparticles into the bloodstream [111]. The protein corona, a dynamic coating of adsorbed serum proteins that spontaneously forms around nanoparticles upon contact with biological fluids, is a critical factor affecting the biological performance and safety of GQDs. This protein coating can radically change the size, charge, and surface chemistry of a nanoparticle and redefine its biological identity and behavior in a fundamental way [112, 113]. This corona fundamentally redefines the biological identity of GQDs, often overriding engineered surface chemistry, thereby facilitating interactions with cells and tissues [114, 115]. Recreating the process of this dynamic corona formation and evolution is extremely complicated but is important to predict the actual GQD action in the body.

The surface charge on GQDs is critical. The negatively charged plasma proteins like fibrinogen and immunoglobulins will be attracted to positively charged GQDs and can be used as a means to induce immune recognition and clearance. In contrast, neutral or negatively charged surfaces, particularly those functionalized with polyethylene glycol (PEG) or other stealth surface functionality, are usually preferential targets to adsorb dysopsonins such as albumin which can extend the circulatory lifetime and inhibit opsonization. At the same time, PEG modification recovers targeting ability of antibody-conjugated nanoparticles by minimizing the protein corona "mask," to ensure that it does not sterically hide the ligands itself. In general, the GQD surface functionalization chemistry, including the nature, density, and distribution of functional groups, as well as the hydrophobicity of basal planes and edges, determines the selective affinity to proteins and the resultant corona fingerprint [116].

After the formation, this corona radically changes GQD behavior in biological systems, covering targeting ligands, changing effective mass, and regulating cellular uptake routes. More importantly, the biological fate of a nanocarrier depends not only on the composition of the adsorbed protein corona but also on the conformational orientation and binding affinity of those proteins. For example, if albumin retains its normal shape on the surface, it binds to standard receptors. If it unfolds, it triggers scavenger receptors that clear the particle as waste. To illustrate, the active targeting efficacy may be diminished by masking targeting moieties (such as antibodies or folate groups) by adsorbed proteins, leading to the internalization of nanoparticles through other non-selective receptor-mediated endogenous pathways or rapid clearance. Besides, corona composition determines biodistribution patterns, immune activation, and its possible toxicity profiles and in vivo coronas are frequently more complex and diverse than in vitro counterparts, which makes it difficult to predict its mechanism [116].

While both experimental and theoretical research confirm that the protein corona alters nanoparticle surface properties, conformation, and membrane interactions, the specific atomic-level mechanisms driving these phenomena remain poorly understood. MD simulations have emerged as a pivotal tool for elucidating the atomic-level mechanisms governing protein corona formation and nanoparticle-membrane interactions. By capturing complex phenomena such as the Vroman effect and competitive protein adsorption, these simulations provide critical theoretical support for experimental observations regarding nanoparticle surface properties and conformational changes. However, achieving quantitative alignment between simulation and in vivo experiments remains challenging due to the immense complexity of biological environments, which include hemodynamic forces, extensive plasma protein diversity, and the structural heterogeneity of cell membranes [117]. Atomistic and coarse-grained MD simulations have shown the interaction between albumin, fibrinogen, immunoglobulins and individual amino acids and graphitic surfaces, the binding sites, orientation selectivity's, conformational changes during adsorption and the influence of nanoparticle curvature on protein-surface interactions. The insights would offer a mechanistic perspective of how the surface properties of GQDs (such as charge patterning, functionalization, and hydrophobicity) tune the formation of corona, protein orientation, and protein stability [118-120].

In order to supplement these simulations and address the complexity of multi-protein corona formation and evolution, researchers are creating multiscale models and machine learning frameworks that predict corona composition using nanoparticle descriptors and protein physicochemical properties. These in silico technologies are able to predict competitive protein binding behaviour, corona behaviour and effect on nanoparticle biological behaviour with prediction accuracies of over 90 percent which can be used to make more accurate predictions of GQD behaviour in vivo [121, 122].

Scaleup-uniformity at large scale: Translating the precise nanoscale properties of GQDs from a computer model to real-world manufacturing isn't straightforward. Achieving the same uniform particle size, surface chemistry, and optical features at a large, GMP-compliant scale is challenging, as every batch can bring subtle but important differences. Industrial processes, no matter how refined, will have difficulties maintaining the tight controls over temperature, mixing, and chemical environment required for perfect reproducibility. These variations mean that the qualities predicted in silico must be validated and tuned through ongoing experimental work to get the consistency needed for pharmaceutical use.

Regulatory path-multifunctional nanomaterial approval: Navigating the regulatory approval process for complex nanomaterials like theranostic GQDs is a major roadblock. Unlike conventional drugs, these materials combine therapy and diagnostics and hence may not fit neatly into existing classifications. Regulators require extensive data to characterize what the product is, how it works, and how reliably it performs those functions. This often means using more rigorous, multi-method analyses to confirm size, composition, drug-loading, and function. The approval path may involve both drug and device regulatory frameworks and always demands that every property and performance characteristic be deeply documented and justified [123, 124].

Stability data-ensuring real-world shelf life: Once a GQD formulation is ready, proving it stays stable over time is crucial before real-world use. Long-term stability isn't just a regulatory requirement, and it is central to ensuring safety and reliable therapeutic effect. Nanoparticles tend to change over time: they might clump together, leak drugs prematurely, or alter surface chemistry, all of which can change how they behave in patients. So, developers need to conduct thorough studies under varying storage conditions, adapting standard pharmaceutical stability protocols (like ICH guidelines) to account for these unique nanoparticle behaviors. Without strong stability data, even a promising formulation may never reach patients [125].

FUTURE DIRECTIONS

The future of computational research to speed-up clinical translation of GQD theranostics requires the transition of computational research to the next generation that is not based on descriptive simulations but on predictive and data-driven discovery. The role of artificial intelligence (AI) and machine learning (ML) in this change will not be only to accelerate calculations, but to create strong quantitative structure-property relationship (QSPR) models. The researchers will be able to predict complex biological behaviors such as cellular uptake efficiency, protein corona composition, and blood circulation half-life by training algorithms on large sets of GQD parameters, including size, zeta potential, surface functionalization patterns, etc., without necessarily having to experimentally measure the desired data [126-130].

Moreover, one of the key steps in this direction is the multi-scale modeling analysis, especially, hybrid quantum mechanics/molecular mechanics (QM/MM) paradigms. Although modern DFT methods can describe electronic properties and MD simulations can capture molecular motion, neither approach alone can provide a complete picture of how a nanocarrier crosses and interacts with a cell. This gap may be addressed with multi-scale models, which will combine the accurate electronic behavior of the drug-GQD interface (QM), with the macroscopic behavior of cell membrane penetration and endosomal escape (MM). This whole picture is fundamental to the design of so-called smart delivery systems that can traverse the tumor microenvironment complexity.

In the future, these enhanced computation results will be used to design combination therapies that are synergistic in which there is a co-delivery of multiple agents that release kinetics to eliminate multidrug resistance [131-134]. This ultimately enables personalized nanomedicine through this convergence of high-throughput AI screening and high-fidelity multi-scale modeling. Computational platforms might in this vision construct patient-specific GQDs-optimizing targeting ligand and drug ratios to be appropriate to the unique tumor biopsy profile of an individual-to maximize therapeutic effect and minimise systemic toxicity [135-137].

CONCLUSION

Breast cancers, especially TNBC still pose a major clinical challenge mainly because of its aggressive characteristics and the lack of identifiable molecular targets for treatment. This review article has brought the emergence of GQDs as a versatile and powerful nanoplatform uniquely suited to meet these challenges into focus. With their high drug loading capacity, tunable fluorescence for imaging and exceptional surface functionalization, GQDs are ideal candidates for the development of next generationtheranostic agents for the concurrent diagnosis and treatment of this complex disease.

Crucially, leapfrogging from a conceptual GQD-based therapy to a clinical reality is being made possible by the indispensable role computational modeling plays. In silico techniques such as DFT and MD simulations have evolved from being merely a supporting tool to becoming a must for the rational design and optimization of these nano systems. These methods are able to give unprecedented information on drug binding, release mechanisms and targeting interactions at a level of detail that is often inaccessible through experimentation alone. As we look to the future, the synergy between advanced computational approaches, including artificial intelligence, and innovative nanomaterials like GQDs, promises to pave the way for a new era of smart, personalized cancer therapies, offering new hope for patients with TNBC.

ACKNOWLEDGMENT

The authors gratefully acknowledge Sri Mata Amritanandamayi Devi (Amma), Chancellor, Amrita Vishwa Vidyapeetham, for her inspiration and for providing financial support for the Article Processing Charges (APC) of this publication.

FUNDING

Nil

Declaration of generative AI in scientific writing

Generative AI and AI-assisted technologies such as Perplexity and Grammarly were utilized to enhance the readability and language of the manuscript. After using this tool, the authors reviewed and edited the content as needed and take full responsibility for the content of the published article.

AUTHORS CONTRIBUTIONS

Jimi K J: Investigation, Methodology, Data curation, Formal analysis, Writing – original draft. Vaishnavi G. Page: Investigation, Data curation, Formal analysis. Abhilash Ravikumar: Supervision, Investigation, Methodology, Writing – review and editing. Amrita Thakur: Investigation, Methodology, Writing – review and editing. Anil Kumar S: Supervision, Conceptualization, Data curation, Formal analysis, Writing – review and editing.

CONFLICT OF INTERESTS

Declared none

REFERENCES

1. Swaminathan H, Saravanamurali K, Yadav SA. Extensive review on breast cancer its etiology, progression, prognostic markers, and treatment. Med Oncol. 2023 Jul 14;40(8):238. doi: 10.1007/s12032-023-02111-9, PMID 37442848.
2. Siegel RL, Miller KD, Wagle NS, Jemal A. Cancer statistics, 2023. CA Cancer J Clin. 2023 Jan;73(1):17-48. doi: 10.3322/caac.21763, PMID 36633525.
3. Sung H, Ferlay J, Siegel RL, Laversanne M, Soerjomataram I, Jemal A et al. Global cancer statistics 2020: GLOBOCAN estimates of incidence and mortality worldwide for 36 cancers in 185 countries. CA Cancer J Clin. 2021 May;71(3):209-49. doi: 10.3322/caac.21660, PMID 33538338.
4. Perou CM, Sørlie T, Eisen MB, van de Rijn M, Jeffrey SS, Rees CA et al. Molecular portraits of human breast tumours. Nature. 2000 Aug 17;406(6797):747-52. doi: 10.1038/35021093, PMID 10963602.
5. Lokhandwala Z, Fahim Khan, Srinivas Nayak Sp, Gunosindhu Chakraborthy. Assessment of prevalence of breast cancer in patients with obesity and evaluating benefits of statin therapy in breast cancer treatment. Asian J Pharm Clin Res. 2025 May;18(5):80-6. doi: 10.22159/ajpcr.2025v18i5.54356.
6. Onitilo AA, Engel JM, Greenlee RT, Mukesh BN. Breast cancer subtypes based on ER/PR and Her2 expression: comparison of clinicopathologic features and survival. Clin Med Res. 2009 Jun;7(1-2):4-13. doi: 10.3121/cmr.2009.825, PMID 19574486, PMCID PMC2705273.
7. Howlader N, Altekruse SF, Li CI, Chen VW, Clarke CA, Ries LA et al. US incidence of breast cancer subtypes defined by joint hormone receptor and HER2 status. J Natl Cancer Inst. 2014 May;106(5):dju055. doi: 10.1093/jnci/dju055, PMID 24777111, PMCID PMC4110475.
8. Verma V, Rn H, Basra SS, Chourey N, Sinha P. Profile of surrogate markers of molecular subtypes using the expression pattern of ER, PR, and HER2/NEU receptors in operable breast cancer. Asian J Pharm Clin Res. 2021:148-51. doi: 10.22159/ajpcr.2021.v14i9.42526.
9. Zagami P, Carey LA. Triple negative breast cancer: pitfalls and progress. npj Breast Cancer. 2022 Aug 20;8(1):95. doi: 10.1038/s41523-022-00468-0, PMID 35987766, PMCID PMC9391239.
10. Xiong N, Wu H, Yu Z. Advancements and challenges in triple-negative breast cancer: a comprehensive review of therapeutic and diagnostic strategies. Front Oncol. 2024 May 28;14:1405491. doi: 10.3389/fonc.2024.1405491, PMID 38863622, PMCID PMC11164589.
11. Goldvaser H, AlGorashi I, Ribnikar D, Seruga B, Templeton AJ, Ocana A et al. Efficacy of extended adjuvant therapy with aromatase inhibitors in early breast cancer among common clinicopathologically-defined subgroups: a systematic review and meta-analysis. Cancer Treat Rev. 2017;60:53-9. doi: 10.1016/j.ctrv.2017.08.008, PMID 28881223.

12. Rimawi MF, De Angelis C, Schiff R. Resistance to anti-HER2 therapies in breast cancer. Am Soc Clin Oncol Educ Book. 2015:e157-64. doi: 10.14694/EdBook_AM.2015.35.e157. PMID 25993167.
13. Ko NR, Nafiujjaman M, Lee JS, Lim HN, Lee YK, Kwon IK. Graphene quantum dot-based theranostic agents for active targeting of breast cancer. RSC Adv. 2017;7(19):11420-7. doi: 10.1039/C6RA25949A.
14. Bianchini G, Balko JM, Mayer IA, Sanders ME, Gianni L. Triple-negative breast cancer: challenges and opportunities of a heterogeneous disease. Nat Rev Clin Oncol. 2016 Nov;13(11):674-90. doi: 10.1038/nrclinonc.2016.66, PMID 27184417.
15. Choi KY, Liu G, Lee S, Chen X. Theranostic nanoplatforms for simultaneous cancer imaging and therapy: current approaches and future perspectives. Nanoscale. 2012;4(2):330-42. doi: 10.1039/C1NR11277E, PMID 22134683, PMCID PMC3269971.
16. Kelkar SS, Reineke TM. Theranostics: combining imaging and therapy. Bioconjug Chem. 2011 Oct 19;22(10):1879-903. doi: 10.1021/bc200151q, PMID 21830812.
17. Nurunnabi M, Khatun Z, Huh KM, Park SY, Lee DY, Cho KJ et al. In vivo biodistribution and toxicology of carboxylated graphene quantum dots. ACS Nano. 2013 Aug 27;7(8):6858-67. doi: 10.1021/nn402043c, PMID 23829293.
18. Schroeder KL, Goreham RV, Nann T. Graphene quantum dots for theranostics and bioimaging. Pharm Res. 2016 Oct;33(10):2337-57. doi: 10.1007/s11095-016-1937-x, PMID 27207272.
19. Liu J, Li R, Yang B. Carbon dots: a new type of carbon-based nanomaterial with wide applications. ACS Cent Sci. 2020 Dec 14;6(12):2179-95. doi: 10.1021/acscentsci.0c01306, PMID 33376780, PMCID PMC7752970.
20. Wang LJ, Cao G, Tu T, Li HO, Zhou C, Hao XJ, et al. A graphene quantum dot with a single electron transistor as an integrated charge sensor. Appl Phys Lett. 2010 Dec 27;97(26):262113. doi: 10.1063/1.3533021.
21. Li M, Chen T, Gooding JJ, Liu J. Review of carbon and graphene quantum dots for sensing. ACS Sens. 2019 Jul 3;4(7):1732-48. doi: 10.1021/acssensors.9b00514, PMID 31267734.
22. Obijiofor OC, Novikov AS. Exploring the role of density functional theory in the design of gold nanoparticles for targeted drug delivery: a systematic review. J Mol Model. 2025 Jul;31(7):186. doi: 10.1007/s00894-025-06405-9, PMID 40493107.
23. Xu X, Liu A, Liu S, Ma Y, Zhang X, Zhang M, et al. Application of molecular dynamics simulation in self-assembled cancer nanomedicine. Biomater Res. 2023 May 4;27(1):39. doi: 10.1186/s40824-023-00386-7, PMID 37143168, PMCID PMC10157803.
24. Farkaš B, de Leeuw NH. A perspective on modelling metallic magnetic nanoparticles in biomedicine: from monometals to nanoalloys and ligand-protected particles. Materials (Basel). 2021 Jun 28;14(13):3611. doi: 10.3390/ma14133611, PMID 34203371, PMCID PMC8279748.
25. Shi J, Kantoff PW, Wooster R, Farokhzad OC. Cancer nanomedicine: progress, challenges and opportunities. Nat Rev Cancer. 2017 Jan;17(1):20-37. doi: 10.1038/nrc.2016.108, PMID 27834398, PMCID PMC5857237.
26. Rosenblum D, Joshi N, Tao W, Karp JM, Peer D. Progress and challenges towards targeted delivery of cancer therapeutics. Nat Commun. 2018 Apr 12;9(1):1410. doi: 10.1038/s41467-018-03705-y, PMID 29650952, PMCID PMC5897340.
27. Wei R, Liu S, Zhang S, Min L, Zhu S. Cellular and extracellular components in tumor microenvironment and their application in early diagnosis of cancers. Anal Cell Pathol (Amst). 2020;2020:6283796. doi: 10.1155/2020/6283796, PMID 32377504, PMCID PMC7655833.
28. Wang L, Wang W, Wang Y, Tao W, Hou T, Cai D, et al. The graphene quantum dots gated nanoplatform for photothermal-enhanced synergetic tumor therapy. Molecules. 2024 Jan 27;29(3):615. doi: 10.3390/molecules29030615, PMID 38338360, PMCID PMC10856938.
29. Soltani M, Ahmadzadeh N, Rajabi S, Besharati N, Khatamian N, Homayouni Tabrizi M. Efficacy of graphene quantum dot-hyaluronic acid nanocomposites containing quinoline for target therapy against cancer cells. Sci Rep. 2025 Mar 12;15(1):8494. doi: 10.1038/s41598-024-81604-7, PMID 40074749.
30. Qi L, Pan T, Ou L, Ye Z, Yu C, Bao B, et al. Biocompatible nucleus-targeted graphene quantum dots for selective killing of cancer cells via DNA damage. Commun Biol. 2021 Feb 16;4(1):214. doi: 10.1038/s42003-021-01713-1, PMID 33594275, PMCID PMC7887119.
31. Qiu J, Zhang R, Li J, Sang Y, Tang W, Rivera Gil P, et al. Fluorescent graphene quantum dots as traceable, pH-sensitive drug delivery systems. Int J Nanomedicine. 2015 Oct 28;10:6709-24. doi: 10.2147/IJN.S91864. PMID 26604747, PMCID PMC4631430.
32. Unidirwade DS, Lade SN, Umekar MJ, Burle SS, Rangari SW. Innovative theranostic potential of graphene quantum dot nanocomposites in breast cancer. Med Oncol. 2025 Aug 4;42(9):404. doi: 10.1007/s12032-025-02948-2, PMID 40760192.
33. Liu H, Deng Z, Zhang Z, Lin W, Zhang M, Wang H. Graphene quantum dots as metal-free nanozymes for chemodynamic therapy of cancer. Matter. 2024 Mar 6;7(3):977-90. doi: 10.1016/j.matt.2023.12.005.
34. Tade RS, Patil PO. Theranostic prospects of graphene quantum dots in breast cancer. ACS Biomater Sci Eng. 2020 Oct 27;6(11):5987-6008. doi: 10.1021/acsbiomaterials.0c01045, PMID 33449670.
35. Deb J, Paul D, Sarkar U. Density functional theory investigation of nonlinear optical properties of T-graphene quantum dots. J Phys Chem A. 2020;124(7):1312-20. doi: 10.1021/acs.jpca.9b10241, PMID 31978308.
36. Bacon M, Bradley SJ, Nann T. Graphene quantum dots. Part Part Syst Charact. 2014 Apr;31(4):415-28. doi: 10.1002/ppsc.201300252.
37. Ritter KA, Lyding JW. The influence of edge structure on the electronic properties of graphene quantum dots and nanoribbons. Nat Mater. 2009 Mar;8(3):235-42. doi: 10.1038/nmat2378, PMID 19219032.
38. Sharma V, Roondhe B, Saxena S, Shukla A. Role of functionalized graphene quantum dots in hydrogen evolution reaction: a density functional theory study. Int J Hydrog Energy. 2022 Dec 25;47(99):41748-58. doi: 10.1016/j.ijhydene.2022.02.161. ijhydene.2022.02.161.
39. Shen J, Zhu Y, Yang X, Li C. Graphene quantum dots: emergent nanolights for bioimaging, sensors, catalysis and photovoltaic devices. Chem Commun (Camb). 2012;48(31):3686-99. doi: 10.1039/C2CC00110A, PMID 22410424.
40. Iannazzo D, Pistone A, Celesti C, Triolo C, Patané S, Giofré SV, et al. A smart nanovector for cancer targeted drug delivery based on graphene quantum dots. Nanomaterials (Basel). 2019 Feb 18;9(2):282. doi: 10.3390/nano9020282, PMID 30781623, PMCID PMC6409978.
41. Zhu S, Song Y, Wang J, Wan H, Zhang Y, Ning Y et al. Photoluminescence mechanism in graphene quantum dots: quantum confinement effect and surface/edge state. Nano Today. 2017 Apr 1;13:10-4. doi: 10.1016/j.nantod.2016.12.006.
42. Sun H, Gao N, Dong K, Ren J, Qu X. Graphene quantum dots-band-aids used for wound disinfection. ACS Nano. 2014 Jun 24;8(6):6202-10. doi: 10.1021/nn501640q, PMID 24870970.
43. Iannazzo D, Ziccarelli I, Pistone A. Graphene quantum dots: multifunctional nanoplatforms for anticancer therapy. J Mater Chem B. 2017;5(32):6471-89. doi: 10.1039/C7TB00747G, PMID 32264412.
44. Luo M, Cheng W, Zeng X, Mei L, Liu G, Deng W. Folic acid-functionalized black phosphorus quantum dots for targeted chemo-photothermal combination cancer therapy. Pharmaceutics. 2019 May 21;11(5):242. doi: 10.3390/pharmaceutics11050242, PMID 31117238, PMCID PMC6572088.
45. Yan Y, Gong J, Chen J, Zeng Z, Huang W, Pu K, et al. Recent advances on graphene quantum dots: from chemistry and physics to applications. Adv Mater. 2019 May;31(21):e1808283. doi: 10.1002/adma.201808283, PMID 30828898.
46. Zhu S, Song Y, Zhao X, Shao J, Zhang J, Yang B. The photoluminescence mechanism in carbon dots (graphene quantum dots, carbon nanodots, and polymer dots): current state and future perspective. Nano Res. 2015 Feb;8(2):355-81. doi: 10.1007/s12274-014-0644-3.
47. Yan X, Cui X, Li LS. Synthesis of large, stable colloidal graphene quantum dots with tunable size. J Am Chem Soc. 2010 May 5;132(17):5944-5. doi: 10.1021/ja1009376, PMID 20377260.

48. Tabish TA, Scotton CJ, Ferguson DC, Lin L, van der Veen AV, Lowry S, et al. Biocompatibility and toxicity of graphene quantum dots for potential application in photodynamic therapy. Nanomedicine (Lond). 2018 Aug;13(15):1923-37. doi: 10.2217/nnm-2018-0018, PMID 30124363.
49. Chong Y, Ma Y, Shen H, Tu X, Zhou X, Xu J et al. The in vitro and in vivo toxicity of graphene quantum dots. BiomaterialsBiomaterials. 2014;35(19):5041-8. doi: 10.1016/j.biomaterials.2014.03.021, PMID 24685264.
50. Zhang M, Wang W, Zhou N, Yuan P, Su Y, Shao M, et al. Near-infrared light triggered photo-therapy, in combination with chemotherapy using magnetofluorescent carbon quantum dots for effective cancer treating. Carbon. 2017 Jul;118:752-64. doi: 10.1016/j.carbon.2017.03.085. carbon.2017.03.085.
51. Younis MR, He G, Lin J, Huang P. Recent advances on graphene quantum dots for bioimaging applications. Front Chem. 2020 Jun 3;8:424. doi: 10.3389/fchem.2020.00424, PMID 32582629, PMCID PMC7286056.
52. Zhao C, Song X, Liu Y, Fu Y, Ye L, Wang N, et al. Synthesis of graphene quantum dots and their applications in drug delivery. J Nanobiotechnology. 2020 Oct 2;18(1):142. doi: 10.1186/s12951-020-00698-z, PMID 33008457, PMCID PMC7532652.
53. Some S, Gwon AR, Hwang E, Bahn GH, Yoon Y, Kim Y, et al. Cancer therapy using ultrahigh hydrophobic drug-loaded graphene derivatives. Sci Rep. 2014 Sep 10;4:6314. doi: 10.1038/srep06314, PMID 25204358, PMCID PMC4158663.
54. Miao W, Shim G, Lee S, Lee S, Choe YS, Oh YK. Safety and tumor tissue accumulation of pegylated graphene oxide nanosheets for co-delivery of anticancer drug and photosensitizer. BiomaterialsBiomaterials. 2013;34(13):3402-10. doi: 10.1016/j.biomaterials.2013.01.010, PMID 23380350.
55. Ruiz V, Pérez-Marquez A, Maudes J, Grande HJ, Murillo N. Enhanced photostability and sensing performance of graphene quantum dots encapsulated in electrospun polyacrylonitrile nanofibrous filtering membranes. Sens Actuators B. 2018 Jun 1;262:902-12. doi: 10.1016/j.snb.2018.02.081. snb.2018.02.081.
56. Ge J, Lan M, Zhou B, Liu W, Guo L, Wang H, et al. A graphene quantum dot photodynamic therapy agent with high singlet oxygen generation. Nat Commun. 2014 Aug 8;5:4596. doi: 10.1038/ncomms5596, PMID 25105845.
57. Sun H, Wu L, Wei W, Qu X. Recent advances in graphene quantum dots for sensing. Mater Today. 2013 Nov 1;16(11):433-42. doi: 10.1016/j.mattod.2013.10.020. mattod.2013.10.020.
58. Latham AP, Levy ES, Sellers BD, Leung DH. Utilizing molecular simulations to examine nanosuspension stability. Pharmaceutics. 2023 Dec 28;16(1):0. doi: 10.3390/pharmaceutics16010050, PMID 38258061, PMCID PMC10820548.
59. Zheng JJ, Li QZ, Wang Z, Wang X, Zhao Y, Gao X. Computer-aided nanodrug discovery: recent progress and future prospects. Chem Soc Rev. 2024;53(18):9059-132. doi: 10.1039/D3CS00575E, PMID 39148378.
60. Abughalia A, Flynn M, Clarke PF, Fayne D, Gobbo OL. The use of computational approaches to design nanodelivery systems. Nanomaterials (Basel). 2025 Sep 3;15(17):1354. doi: 10.3390/nano15171354, PMID 40938032.
61. Mitchell MJ, Billingsley MM, Haley RM, Wechsler ME, Peppas NA, Langer R. Engineering precision nanoparticles for drug delivery. Nat Rev Drug Discov. 2021 Feb;20(2):101-24. doi: 10.1038/s41573-020-0090-8, PMID 33277608.
62. Herdiana Y. Bridging the gap: the role of advanced formulation strategies in the clinical translation of nanoparticle-based drug delivery systems. Int J Nanomedicine. 2025 Dec 31;20:13039-53. doi: 10.2147/IJN.S554821. PMID 41185748, PMCID PMC10948902.
63. Shukla S, Jakowski J, Kadian S, Narayan RJ. Computational approaches to delivery of anticancer drugs with multidimensional nanomaterials. Comput Struct Biotechnol J. 2023 Jan 1;21:4149-58. doi: 10.1016/j.csbj.2023.08.010. PMID 37675288, PMCID PMC10439829.
64. Matyszczak G, Krawczyk K, Yedzikhanau A. Computational modeling of properties of quantum dots and nanostructures: from first principles to artificial intelligence (A review). Nanomaterials (Basel). 2025 Feb 11;15(4):272. doi: 10.3390/nano15040272, PMID 39997835.
65. Kumar A, Sayyed MI, Punina D, Naranjo E, Jácome E, Abdulameer MK, et al. Graphene quantum dots (GQD) and edge-functionalized GQDs as hole transport materials in perovskite solar cells for producing renewable energy: a DFT and TD-DFT study. RSC Adv. 2023;13(42):29163-73. doi: 10.1039/D3RA05438A, PMID 37800128, PMCID PMC10544785.
66. Feng J, Guo Q, Song N, Liu H, Dong H, Chen Y, et al. Density functional theory study on optical and electronic properties of co-doped graphene quantum dots based on different nitrogen doping patterns. Diam Relat Mater. 2021 Mar 1;113:108264. doi: 10.1016/j.diamond.2021.108264.
67. Edet HO, Louis H, Gber TE, Idante PS, Egemonye TC, Ashishie PB, et al. Heteroatoms (B, N, S) doped quantum dots as potential drug delivery system for isoniazid: insight from DFT, NCI, and QTAIM. Heliyon. 2023 Jan;9(1):e12599. doi: 10.1016/j.heliyon.2022.e12599, PMID 36691540, PMCID PMC9850111.
68. Opi MH, Ahmed T, Swarna MR, Piya AA, Shamim SU. Assessment of the drug delivery potential of graphene, boron nitride and their in-plane doped structures for hydroxyurea anti-cancer drug via DFT study. Nanoscale Adv. 2024;6(20):5042-54. doi: 10.1039/D4NA00428K, PMID 39148501, PMCID PMC11259235.
69. Björk J, Hanke F, Palma CA, Samori P, Cecchini M, Persson M. Adsorption of aromatic and anti-aromatic systems on graphene through π–π stacking. J Phys Chem Lett. 2010 Dec 2;1(23):3407-12. doi: 10.1021/jz101360k.
70. Feng J, Dong H, Yu L, Dong L. The optical and electronic properties of graphene quantum dots with oxygen-containing groups: a density functional theory study. J Mater Chem C. 2017;5(24):5984-93. doi: 10.1039/C7TC00631D.
71. Zhao Y, Truhlar DG. The M06 suite of density functionals for main group thermochemistry, thermochemical kinetics, noncovalent interactions, excited states, and transition elements: two new functionals and systematic testing of four M06-class functionals and 12 other functionals. Theor Chem Account. 2008 May;120(1-3):215-41. doi: 10.1007/s00214-007-0310-x.
72. Grimme S. Semiempirical GGA-type density functional constructed with a long-range dispersion correction. J Comput Chem. 2006 Nov 30;27(15):1787-99. doi: 10.1002/jcc.20495, PMID 16955487.
73. Grimme S, Ehrlich S, Goerigk L. Effect of the damping function in dispersion corrected density functional theory. J Comput Chem. 2011 May;32(7):1456-65. doi: 10.1002/jcc.21759, PMID 21370243.
74. Goerigk L, Grimme S. A thorough benchmark of density functional methods for general main group thermochemistry, kinetics, and noncovalent interactions. Phys Chem Chem Phys. 2011;13(14):6670-88. doi: 10.1039/C0CP02984J, PMID 21384027.
75. Zhang Y, Wang JG, Wang W. Noncovalent interactions between 1,3,5-trifluoro-2,4,6-triiodobenzene and a series of 1,10-phenanthroline derivatives: A combined theoretical and experimental study. Crystals. 2019 Mar 8;9(3):140. doi: 10.3390/cryst9030140.
76. Weigend F, Ahlrichs R. Balanced basis sets of split valence, triple zeta valence and quadruple zeta valence quality for H to Rn: design and assessment of accuracy. Phys Chem Chem Phys. 2005;7(18):3297-305. doi: 10.1039/B508541A, PMID 16240044.
77. Yoosefian M, Fouladi M, Atanase LI. Molecular dynamics simulations of docetaxel adsorption on graphene quantum dots surface modified by PEG-b-PLA copolymers. Nanomaterials (Basel). 2022 Mar 11;12(6):926. doi: 10.3390/nano12060926, PMID 35335739, PMCID PMC8955342.
78. Wolski P. Molecular Dynamics simulations of the pH-dependent adsorption of doxorubicin on carbon quantum dots. Mol Pharm. 2020;18(1):257-66. doi: 10.1021/acs.molpharmaceut.0c00895, PMID 33325232.
79. Zhang P, Jiao F, Wu L, Kong Z, Hu W, Liang L et al. Molecular dynamics simulation of transport mechanism of graphene quantum dots through different cell membranes. Membranes (Basel). 2022 Jul 31;12(8):753. doi: 10.3390/membranes12080753, PMID 36005668, PMCID PMC9416039.
80. Kong Z, Zhang P, Chen J, Zhou H, Ma X, Wang H et al. Effect of shape on the entering of graphene quantum dots into a membrane: a molecular dynamics simulation. ACS Omega. 2021 Apr 16;6(16):10936-43. doi: 10.1021/acsomega.1c00689, PMID 34056246, PMCID PMC8156329.

81. Jorgensen WL, Maxwell DS, Tirado-Rives J. Development and testing of the OPLS all-atom force field on conformational energetics and properties of organic liquids. J Am Chem Soc. 1996 Nov 13;118(45):11225-36. doi: 10.1021/ja9621760.
82. Case DA, Aktulga HM, Belfon K, Cerutti DS, Cisneros GA, Cruzeiro VW et al. AmberTools. J Chem Inf Model. 2023 Oct 23;63(20):6183-91. doi: 10.1021/acs.jcim.3c01153. PMID 37805934, PMCID PMC10598796.
83. MacKerell AD Jr, Bashford D, Bellott M, Dunbrack RL Jr, Evanseck JD, Field MJ, et al. All-atom empirical potential for molecular modeling and dynamics studies of proteins. J Phys Chem B. 1998 Apr 30;102(18):3586-616. doi: 10.1021/jp973084f, PMID 24889800.
84. van Duin AC, Dasgupta S, Lorant F, Goddard WA 3rd. ReaxFF: a reactive force field for hydrocarbons. J Phys Chem A. 2001 Oct 18;105(41):9396-409. doi: 10.1021/jp004368u.
85. Sousa CF, Becker RA, Lehr CM, Kalinina OV, Hub JS. Simulated tempering-enhanced umbrella sampling improves convergence of free energy calculations of drug membrane permeation. J Chem Theory Comput. 2023 Feb 28;19(6):1898-907. doi: 10.1021/acs.jctc.2c01162. PMID 36853966, PMCID PMC10408274.
86. Alinejad A, Raissi H, Hashemzadeh H. Understanding co-loading of doxorubicin and camptothecin on graphene and folic acid-conjugated graphene for targeting drug delivery: classical MD simulation and DFT calculation. J Biomol Struct Dyn. 2020 Jun 12;38(9):2737-45. doi: 10.1080/07391102.2019.1645044, PMID 31311443.
87. Sawy AM, Barhoum A, Abdel Gaber SA, El-Hallouty SM, Shousha WG, Maarouf AA et al. Insights of doxorubicin loaded graphene quantum dots: synthesis, DFT drug interactions, and cytotoxicity. Mater Sci Eng C Mater Biol Appl. 2021 Mar 1;122:111921. doi: 10.1016/j.msec.2021.111921. PMID 33641914.
88. Vatanparast M, Shariatinia Z. AlN and AlP doped graphene quantum dots as novel drug delivery systems for 5-fluorouracil drug: theoretical studies. J Fluor Chem. 2018 Jul 1;211:81-93. doi: 10.1016/j.jfluchem.2018.04.003.
89. Vatanparast M, Shariatinia Z. Revealing the role of different nitrogen functionalities in the drug delivery performance of graphene quantum dots: a combined density functional theory and molecular dynamics approach. J Mater Chem B. 2019;7(40):6156-71. doi: 10.1039/C9TB00971J, PMID 31559403.
90. Munny KN, Ahmed T, Piya AA, Shamim SU. Exploring the adsorption performance of doped graphene quantum dots as anticancer drug carriers for cisplatin by DFT, PCM, and COSMO approaches. Struct Chem. 2023 Dec;34(6):2089-105. doi: 10.1007/s11224-023-02150-y.
91. Mahdavi M, Rahmani F, Nouranian S. Molecular simulation of pH-dependent diffusion, loading, and release of doxorubicin in graphene and graphene oxide drug delivery systems. J Mater Chem B. 2016;4(46):7441-51. doi: 10.1039/C6TB00746E, PMID 32263744.
92. Özönder Ş, Ünlü C, Güleryüz C, Trabzon L. Doped graphene quantum dots UV–vis absorption spectrum: a high-throughput TDDFT study. ACS Omega. 2023 Jan 5;8(2):2112-8. doi: 10.1021/acsomega.2c06091, PMID 36687068, PMCID PMC9851777.
93. Kansara V, Tiwari S, Patel M. Graphene quantum dots: a review on the effect of synthesis parameters and theranostic applications. Colloids Surf B Biointerfaces. 2022;217:112605. doi: 10.1016/j.colsurfb.2022.112605, PMID 35688109.
94. Drissi LB, Ouarrad H, Ramadan FZ, Fritzsche W. Graphene and silicene quantum dots for nanomedical diagnostics. RSC Adv. 2020;10(2):801-11. doi: 10.1039/C9RA08399E, PMID 35494439, PMCID PMC9048619.
95. Nhan DT, Van Bay M, Nhung NT, Hien NK, Quang DT. Investigation of excitation and emission properties of fluorescence compounds by DFT and TD-DFT methods. Hue Univ J Sci Nat Sci. 2018 May 9;127(1A):43-53. doi: 10.26459/hueuni-jns. v127i1A.4777.
96. Elkabiri K, Ouarrad H, Drissi LB. Development of advanced drug-loaded graphene quantum dots with improved photoluminescence properties for enhanced targeted therapy and nano-imaging technologies. RSC Adv. 2025;15(17):13561-73. doi: 10.1039/D4RA07998A, PMID 40297001.
97. Elkabiri K, Ouarrad H, Drissi LB. Engineering mitoxantrone-conjugated graphene quantum dots for advanced photoluminescent cancer therapy. Mater Sci Semicond Process. 2025 Feb 1;186:109066. doi: 10.1016/j.mssp.2024.109066.
98. El-Sayed NM, Elhaes H, Ibrahim A, Ibrahim MA. Investigating the electronic properties of edge glycine/biopolymer/graphene quantum dots. Sci Rep. 2024 Sep 20;14(1):21973. doi: 10.1038/s41598-024-71655-1, PMID 39304667, PMCID PMC10765447.
99. Bhaloo A, Nguyen S, Lee BH, Valimukhametova A, Gonzalez-Rodriguez R, Sottile O, et al. Doped graphene quantum dots as biocompatible radical scavenging agents. Antioxidants (Basel). 2023 Jul 31;12(8):1536. doi: 10.3390/antiox12081536, PMID 37627531, PMCID PMC10451151.
100. Akbari M. Interaction of some phytochemical compounds with Er2O3 nanoparticle: first principle study. J Mol Model. 2025 May;31(5):132. doi: 10.1007/s00894-025-06361-4, PMID 40178631.
101. Valimukhametova AR, Fannon O, Topkiran UC, Dorsky A, Sottile O, Gonzalez-Rodriguez R, et al. Five near-infrared-emissive graphene quantum dots for multiplex bioimaging. 2D Mater. 2024 Jan 19;11(2):025009. doi: 10.1088/2053-1583/ad1c6e, PMID 39149578.
102. Rasheed PA, Ankitha M, Pillai VK, Alwarappan S. Graphene quantum dots for biosensing and bioimaging. RSC Adv. 2024;14(23):16001-23. doi: 10.1039/d4ra01431f, PMID 38765479, PMCID PMC11127529.
103. Bianco A. Graphene: safe or toxic? The two faces of the medal. Angew Chem Int Ed Engl. 2013 May 3;52(19):4986-97. doi: 10.1002/anie.201209099, PMID 23580235.
104. Kong Z, Hu W, Jiao F, Zhang P, Shen J, Cui B et al. Theoretical evaluation of DNA genotoxicity of graphene quantum dots: A combination of density functional theory and Molecular Dynamics simulations. J Phys Chem B. 2020;124(42):9335-42. doi: 10.1021/acs.jpcb.0c05882, PMID 32870004.
105. Liang L, Shen X, Zhou M, Chen Y, Lu X, Zhang L et al. Theoretical evaluation of potential cytotoxicity of graphene quantum dot to adsorbed DNA. Materials (Basel). 2022 Oct 23;15(21):7435. doi: 10.3390/ma15217435, PMID 36363026, PMCID PMC9655443.
106. Nilewski L, Mendoza K, Jalilov AS, Berka V, Wu G, Sikkema WK, et al. Highly oxidized graphene quantum dots from coal as efficient antioxidants. ACS Appl Mater Interfaces. 2019 Apr 17;11(18):16815-21. doi: 10.1021/acsami.9b01082, PMID 30995006.
107. Ku TH, Shen WT, Hsieh CT, Chen GS, Shia WC. Specific forms of graphene quantum dots induce apoptosis and cell cycle arrest in breast cancer cells. Int J Mol Sci. 2023 Feb 17;24(4):4046. doi: 10.3390/ijms24044046, PMID 36835458, PMCID PMC9967131.
108. Gunes BA, Kirlangic OF, Kilic M, Sunguroglu A, Ozgurtas T, Sezginer EK, et al. Palladium metal nanocomposites based on PEI-functionalized nitrogen-doped graphene quantum dots: synthesis, characterization, density functional theory modeling, and cell cycle arrest effects on human ovarian cancer cells. ACS Omega. 2024 Mar 6;9(11):13342-58. doi: 10.1021/acsomega.3c10324, PMID 38524449, PMCID PMC10958141.
109. Jayasinghe MK, Lee CY, Tran TT, Tan R, Chew SM, Yeo BZ, et al. The role of in silico research in developing nanoparticle-based therapeutics. Front Digit Health. 2022 Mar 16;4:838590. doi: 10.3389/fdgth.2022.838590, PMID 35373184, PMCID PMC8972619.
110. Stillman NR, Kovacevic M, Balaz I, Hauert S. In silico modelling of cancer nanomedicine, across scales and transport barriers. npj Comput Mater. 2020 Jul 8;6(1):92. doi: 10.1038/s41524-020-00366-8.
111. Lee H. Recent advances in simulation studies on the protein corona. Pharmaceutics. 2024 Nov 6;16(11):1419. doi: 10.3390/pharmaceutics16111419, PMID 39598542, PMCID PMC11306364.
112. Marques C, Borchard G, Jordan O. Unveiling the challenges of engineered protein corona from the proteins' perspective. Int J Pharm. 2024;654:123987. doi: 10.1016/j.ijpharm.2024.123987, PMID 38467206.
113. Docter D, Westmeier D, Markiewicz M, Stolte S, Knauer SK, Stauber RH. The nanoparticle biomolecule corona: lessons learned – challenge accepted? Chem Soc Rev. 2015;44(17):6094-121. doi: 10.1039/C5CS00217F, PMID 26065524.

114. Rampado R, Crotti S, Caliceti P, Pucciarelli S, Agostini M. Recent advances in understanding the protein corona of nanoparticles and in the formulation of "stealthy" nanomaterials. Front Bioeng Biotechnol. 2020 Apr 3;8:166. doi: 10.3389/fbioe.2020.00166, PMID 32309278, PMCID PMC7147453.
115. Park SJ. Protein–nanoparticle interaction: corona formation and conformational changes in proteins on nanoparticles. Int J Nanomedicine. 2020 Aug 6;15:5783-802. doi: 10.2147/IJN.S254808. PMID 32821101, PMCID PMC7424350.
116. Fleischer CC, Payne CK. Secondary structure of corona proteins determines the cell surface receptors used by nanoparticles. J Phys Chem B. 2014 Dec 11;118(49):14017-26. doi: 10.1021/jp502624n, PMID 24779411, PMCID PMC4311548.
117. Lee H. Molecular modeling of protein corona formation and its interactions with nanoparticles and cell membranes for nanomedicine applications. Pharmaceutics. 2021 Apr 29;13(5):637. doi: 10.3390/pharmaceutics13050637, PMID 33947090, PMCID PMC8146999.
118. Ye J, Fan M, Zhan J, Zhang X, Lu S, Chai M et al. In silico bioactivity prediction of proteins interacting with graphene-based nanomaterials guides rational design of biosensor. TalantaTalanta. 2024;277:126397. doi: 10.1016/j.talanta.2024.126397, PMID 38865956.
119. Panczyk T, Nieszporek J, Nieszporek K. Molecular dynamics simulations of interactions between human telomeric I-motif deoxyribonucleic acid and functionalized graphene. J Phys Chem B. 2022 Aug 29;126(35):6671-81. doi: 10.1021/acs.jpcb.2c04327. PMID 36036695, PMCID PMC9455338.
120. Huang W, Wang Z, Luo J. Molecular Dynamics study of the curvature-driven interactions between carbon-based nanoparticles and amino acids. Molecules. 2023 Jan 4;28(2):482. doi: 10.3390/molecules28020482, PMID 36677540, PMCID PMC9865351.
121. Huzar J, Coreas R, Landry MP, Tikhomirov G. AI-Based prediction of protein corona composition on DNA nanostructures. ACS Nano. 2025 Jan 8;19(4):4333-45. doi: 10.1021/acsnano.4c12259, PMID 39772513.
122. Canchola A, Li K, Chen K, Borboa-Pimentel A, Chou C, Dela Rama R, et al. Meta-analysis and machine learning prediction of protein corona composition across nanoparticle systems in biological media. ACS Nano. 2025 Oct 1;19(43):37633-50. doi: 10.1021/acsnano.5c08608, PMID 41031442.
123. Kapoor S, Jha A, Ahmad H, Islam SS. Avenue to large-scale production of graphene quantum dots from high-purity graphene sheets using laboratory-grade graphite electrodes. ACS Omega. 2020 Jul 22;5(30):18831-41. doi: 10.1021/acsomega.0c01993, PMID 32775885, PMCID PMC7399303.
124. Hua S, de Matos MB, Metselaar JM, Storm G. Current trends and challenges in the clinical translation of nanoparticulate nanomedicines: pathways for translational development and commercialization. Front Pharmacol. 2018 Jul 17;9:790. doi: 10.3389/fphar.2018.00790, PMID 30065653, PMCID PMC6056682.
125. Punnakkal N, Naneena S, C P SL, Pradeep A, T G SB, Suneesh PV. Nitrogen-doped graphene quantum dot embedded polyaniline for the fabrication of high-performance flexible supercapacitor with enhanced cycling stability. J Energy Storage. 2024;100:113527. doi: 10.1016/j.est.2024.113527.
126. Krishnakumar S, Paul V, Ariyath A, Anoop PD, Sreekumar S, Menon D, et al. Graphene quantum dots alter proliferation and meiosis of germ cells only in genetic females of Japanese medaka during early embryonic development. ACS Appl Bio Mater. 2019 Feb 18;2(2):737-46. doi: 10.1021/acsabm.8b00606, PMID 35016278.
127. Wang Q, Liu Y, Li C, Xu B, Xu S, Liu B. Machine learning-enhanced nanoparticle design for precision cancer drug delivery. Adv Sci (Weinh). 2025;12(30):e03138. doi: 10.1002/advs.202503138, PMID 40536233.
128. Xu Y, Dai Z, Chen F, Gao S, Pei J, Lai L. Deep learning for drug-induced liver injury. J Chem Inf Model. 2015;55(10):2085-93. doi: 10.1021/acs.jcim.5b00238, PMID 26437739.
129. Chen H, Engkvist O, Wang Y, Olivecrona M, Blaschke T. The rise of deep learning in drug discovery. Drug Discov Today. 2018 Jun;23(6):1241-50. doi: 10.1016/j.drudis.2018.01.039. PMID 29366762.
130. Omidian H, Wilson RL, Cubeddu LX. Quantum dot research in breast cancer: challenges and prospects. Materials (Basel). 2024 May 4;17(9):2152. doi: 10.3390/ma17092152, PMID 38730959, PMCID PMC11085569.
131. Pareek A, Kumar D, Pareek A, Gupta MM. Advancing cancer therapy with quantum dots and other nanostructures: a review of drug delivery innovations, applications, and challenges. Cancers (Basel). 2025 Mar 4;17(5):878. doi: 10.3390/cancers17050878, PMID 40075725.
132. Yang D, Yao X, Dong J, Wang N, Du Y, Sun S et al. Design and investigation of core/shell GQDs/hMSN nanoparticles as an enhanced drug delivery platform in triple-negative breast cancer. Bioconjug Chem. 2018;29(8):2776-85. doi: 10.1021/acs.bioconjchem.8b00399, PMID 30011184.
133. Tian Z, Yao X, Ma K, Niu X, Grothe J, Xu Q et al. Metal–organic framework/graphene quantum dot nanoparticles used for synergistic chemo- and photothermal therapy. ACS Omega. 2017 Mar 1;2(3):1249-58. doi: 10.1021/acsomega.6b00385, PMID 30023630, PMCID PMC6640740.
134. Campbell E, Hasan MT, Gonzalez-Rodriguez R, Truly T, Lee BH, Green KN et al. Graphene quantum dot formulation for cancer imaging and redox-based drug delivery. Nanomedicine. 2021 Oct;37:102408. doi: 10.1016/j.nano.2021.102408. PMID 34015513, PMCID PMC9237544.
135. Hare JI, Lammers T, Ashford MB, Puri S, Storm G, Barry ST. Challenges and strategies in anti-cancer nanomedicine development: an industry perspective. Adv Drug Deliv Rev. 2017;108:25-38. doi: 10.1016/j.addr.2016.04.025, PMID 27137110.
136. Duncan R, Gaspar R. Nanomedicine(s) under the microscope. Mol Pharm. 2011 Dec 5;8(6):2101-41. doi: 10.1021/mp200394t, PMID 21974749.
137. Kumari S. Diferuloylmethane identified against cysteine proteases and TMPRSS2 using an *in silico* approach. Int J Chem Res. 2025;9(3):9-15. doi: 10.22159/ijcr.2025v9i3.270.